Precambrian Research 321 (2019) 349–374

Contents lists available at ScienceDirect

Precambrian Research

journal homepage: www.elsevier.com/locate/precamres

Organic-walled microfossils from the late Mesoproterozoic to early Neoproterozoic lower Shaler Supergroup (Arctic Canada): Diversity and biostratigraphic significance

Corentin C. Loron[a,*], Robert H. Rainbird[b], Elizabeth C. Turner[c], J. Wilder Greenman[d], Emmanuelle J. Javaux[a]

[a] Department of Geology, University of Liège, Liège, Belgium
[b] Geological Survey of Canada Ottawa, ON, Canada
[c] Harquail School of Earth Sciences, Laurentian University, Sudbury, ON, Canada
[d] Department of Earth and Planetary Sciences, McGill University, QC, Canada

ARTICLE INFO

Keywords:
Organic-walled microfossils
Eukaryotes
Shaler Supergroup
Canada
Mesoproterozoic
Neoproterozoic

ABSTRACT

The diversification of acritarchs (organic-walled vesicular microfossils of unknown affinity), filamentous, and multicellular microorganisms, happened during a time of profound environmental, biological, and ecological change. The Mesoproterozoic to Neoproterozoic transition is a key interval, notably for eukaryotic organisms. New assemblages of organic-walled microfossils from the ca. 1230 Ma to 900 Ma lower Shaler Supergroup of Arctic Canada record an impressive diversity, including macroscopic compressions of *Chuaria circularis* and numerous unambiguous eukaryotic taxa. The index taxon *Trachyhystrichosphaera aimika* co-occurs with eukaryotic taxa hitherto reported only from earlier (*Dictyosphaera, Gigantosphaeridium, Satka favosa – sensu* Javaux and Knoll, 2016) or later (*Microlepidopalla)* time intervals. Five new taxa, comprising the spheroidal acritarchs with inner wall sculpture *Nunatsiaquus cryptotorus* n. gen., n. sp. and *Daedalosphaera digitisigna* n. gen., n. sp.; the acanthomorphs (spiny acritarchs) with regularly distributed processes *Herisphaera arbovela* n. gen., n. sp. and *Herisphaera triangula* n. sp.; and the process-bearing multicellular *Ourasphaira giraldae* n. gen., n. sp.; are reported, along with three unnamed forms. Collectively, these remarkable microfossils (63 taxa, including 25 eukaryotic forms) demonstrate the greatest diversity of eukaryotes ever recorded for this time interval.

1. Introduction

The Proterozoic Era is a time of significant changes in Earth's biosphere, especially for the eukaryotic domain (Javaux, 2011; Butterfield 2015a; Knoll, 2015; Javaux and Lepot, 2017). The rise in morphological complexity and diversity documented by paleontological data (Butterfield; 1997; 2015a,b; Huntley et al., 2006; Knoll et al., 2006; Agić et al., 2015; 2017; Cohen and Macdonald, 2015; Javaux and Knoll, 2016; Baludikay et al., 2016; Adam et al., 2017; Beghin et al., 2017a; Riedman and Sadler, 2017; Riedman et al., 2018; Xiao and Tang, 2018) took place from the late Paleoproterozoic through the Neoproterozoic. This important transition coincides with physico-chemical changes in Earth's atmosphere and ocean, volcanism, and tectonics (e.g. Lyons et al, 2014; Lenton et al., 2014; Planavsky et al., 2014; Javaux and Lepot, 2017), but also with biological innovations (Javaux, 2006, 2011; Javaux and Knoll, 2016; Knoll and Lahr, 2016). Such innovations include the development of different types of reproduction (Javaux, 2006, 2011; Agić et al., 2015), the appearance of multicellularity (Butterfield 2009; Knoll and Lahr, 2016; Javaux and Knoll, 2016), the acquisition of chloroplasts and the appearance of crown group eukaryotes with variable minimum age estimates (e.g. red algae (Butterfield, 2000; Bengston et al., 2017; but see Gibson et al., 2017) and green algae (Arouri et al., 1999; Marshall et al., 2005; Xiao and Dong, 2006; Moczydłowska and Willman, 2009; Moczydłowska 2016; Brocks et al., 2017); testate amoebae (Porter and Knoll, 2000; Porter et al., 2003; Morais et al., 2017; Riedman et al., 2018); foraminifera (Bosak et al., 2011a,b) and possible ciliates (Bosak et al., 2012); biomineralisation (Cohen et al., 2011); and the evolution of predation by protists on protists (Porter, 2011, 2016; Knoll and Lahr, 2016; Loron et al., 2018; Cohen and Riedman, 2018)).

Attempts to resolve the diversification pattern of eukaryotes through the Precambrian suffer from numerous taphonomic and

* Corresponding author.
E-mail address: c.loron@uliege.be (C.C. Loron).

https://doi.org/10.1016/j.precamres.2018.12.024
Received 27 April 2018; Received in revised form 27 November 2018; Accepted 19 December 2018
Available online 21 December 2018

sampling biases (Knoll et al., 2006; Cohen and Macdonald, 2015) that may be reduced by investigating new assemblages and re-studying previously studied successions.

Recent investigations of assemblages from Africa, Australia, China, India, and Laurentia have improved our understanding of fossil diversity in the Mesoproterozoic and early Neoproterozoic (Agić et al., 2015; 2017; Javaux and Knoll, 2016; Baludikay et al., 2016; Beghin et al., 2017a; Tang et al., 2017). The diverse, well-preserved organic-walled microfossils presented in these studies show that eukaryotes were already thriving prior to the major mid-Neoproterozoic expansion of the domain, as previously predicted in a model based on the appearance of biological innovations and of stem and crown-group eukaryotes (Javaux, 2011).

The geology and geochronology of the Shaler Supergroup, in Arctic Canada, is well documented (Young et al., 1979; 1981; Lecheminant and Heaman, 1989; Heaman et al., 1992; Rainbird et al., 1992; 1994; 1996; 2018; Rayner and Rainbird, 2013; Van Acken et al., 2013). The Wyniatt Formation, in the upper ShalerSupergroup, yielded a variety of micro- and macrofossils (Hofmann and Rainbird, 1994; Butterfield and Rainbird, 1998; Butterfield, 2005a,b), but the Boot Inlet, Grassy Bay, Aok, Nelson Head, Mikkelsen Island and Escape Rapids formations, in the lower part of the succession remained uninvestigated for paleontology (except for a few taxa with predation marks, Loron et al, 2018).

We investigated the fossil diversity of marine siliciclastic and carbonate rocks of the lower Shaler Supergroup, which were deposited at < 1.2 – 0.9 Ga (Rainbird et al., 1996; 2018). Prior to this study, the highest eukaryotic diversity in contemporaneous assemblages was reported from the Atar/El Mreïti Group, Mauritania, and the Mbuji-Mayi Supergroup, RDC, with 11 species of unambiguous eukaryotes for each succession (Baludikay et al., 2016; Beghin et al., 2017a) but the lower Shaler Supergroup preserves an unprecedented eukaryote diversity from this time in Earth history, with 25 taxa.

The present material includes macroscopic compressions, spheroidal vesicles with inner wall sculpture, spheroidal vesicles with smooth wall surface, process-bearing (acanthomorphic) microfossils, multicellular taxa. Five new species of organic-walled microfossils are described. Some of the taxa were previously considered characteristic of other younger or older time intervals, so their presence has significant implications for the biostratigraphy and pattern of early eukaryote diversification.

2. Geological background

2.1. The Shaler Supergroup

The geological successions of northwestern Laurentia are subdivided into large scale, unconformity-bounded sequences that can be broadly correlated across northwestern Canada (Young et al., 1979; Young, 1981; Rainbird et al., 1996; Long et al., 2008). In stratigraphic order, these sequences are referred to as: A (> 1.08 Ma), B (0.72 – 1.08 Ma) and C (0.54 – 0.72 Ma). The Shaler Supergroup, in northwestern Canada, is comprised within Sequence A to upper Sequence B and unconformably overlies the Coppermine River Group in the Coppermine area. The top of the Shaler Supergroup is constrained by the 0.72 Ga Natkusiak Formation flood basalt, marking the boundary between Sequence B and C (Fig. 1) (Rainbird et al., 1996).

The Shaler Supergroup rocks crop out in the Minto and Duke of York inliers on Victoria Island, in the Cape Lambton inlier on southern Banks Island, and, on the mainland, in the Brock inlier and Coppermine areas (Fig. 1). The ~5 km-thick succession is an alternation of carbonate rocks and sandstone, with subordinate shale, siltstone, and mudstone (Fig. 1), deposited in the Amundsen basin, in an intracontinental sea that was episodically connected to an open ocean (Rainbird et al., 1996).

The Grassy Bay and Nelson Head formations mainly indicate deposition in fluvial to marine deltaic environments, whereas the Boot Inlet, Aok, Mikkelsen Islands and Escape Rapids formations record shallow sub- to intertidal marine settings. The top of the Nelson Head Formation is interpreted to represent deposition on a high-energy reworked delta, and marine shoreface environment (Greenman and Rainbird, 2018). The Nelson Head and Grassy Bay formations are correlated with the Katherine Group and Tsezotene Formation from the Mackenzie Mountains Supergroup, located approximately 500 km southwest of the Brock inlier (Long et al., 2008).

2.2. Age of the lower Shaler Supergroup

The age of the lower Shaler Supergroup is constrained by rhenium-osmium isochron dating of black shale, which provides a minimum age of 892 ± 13 Ma for the upper Boot Inlet Formation (Van Acken et al., 2013; Fig. 1). Uranium-lead dating of detrital zircon grains from fluvial quartz arenite of the Nelson Head Formation and from quartz arenite in the Fort Collinson Formation provide a maximum depositional age of 1013 ± 25 Ma and 891 ± 22 Ma, respectively (Rayner and Rainbird, 2013; Rainbird et al., 2018). A quartz arenite from the middle Escape Rapids Formation yields a maximum depositional age of 1151 ± 13 Ma. In addition, a maximum depositional age by (detrital zircon) of 1232 ± 15 Ma is derived from lithic wacke of the Husky Creek Formation (Coppermine River Group), which unconformably underlies the Escape Rapids Formation (Rayner and Rainbird, 2013; Fig. 1). Thus the fossiliferous assemblages described in this paper were deposited between ca. 1232 Ma and 892 Ma. In addition, samples from Nelson Head and Grassy Bay formations, which record the highest eukaryotic diversity and the new species recovered in this study, can be further constrained to > 1013 – 892 ± 13 Ma, embracing the Mesoproterozoic – Neoproterozoic transition.

3. Material and methods

The rock samples were collected from outcrops and drill cores in the lower part of the Shaler Supergroup, from the Escape Rapids, Nelson Head and Aok formations of the Rae Group and the Grassy Bay and Boot Inlet formations of the Reynolds Point Group (black dots in Fig. 1; see supplementary file for locations) during field expeditions in the Brock Inlier and Coppermine areas in 2014, 2015 and 2017. Samples were macerated in hydrochloric and hydrofluoric acids in the Early Life Traces and Evolution-Astrobiology laboratory of University of Liège (Belgium), following the low-manipulation and low-agitation protocol established by Grey (1999). The kerogenous residue obtained from acid treatments was filtered using 25 µm and 10 µm mesh-size filters. The macerates were mounted on microscope slides and examined under an optical microscope. Transmitted-light photographs were acquired using an Axio Imager A1m microscope equipped with an AxioCam MRc5 digital camera (Carl Zeiss, Germany). In the present work, 26 samples out of 29 preserved microfossils.

Specimens for Scanning Electron Microscopy (SEM) are cover in gold using a Quorum q150T ES and the pictures are acquired using an Auriga microscope (Carl Zeiss, Germany) at the Institut de Physique du Globe de Paris (IPGP), Paris, France.

In the systematics (Section 7), microfossils are described following the International Code of Nomenclature for Algae, Fungi, and Plants; Shenzen 2017. Only new taxa and revised taxa are described in detail here. All taxa from the lower Shaler Supergroup are illustrated on Figs. 2–8 and discussed, with the exception of filamentous taxa that are informally described below and illustrated on Fig. 3. These taxa, conventionally organized in size-class species and abundantly described in the literature (see below) (*Siphonophycus* spp., *Oscillatoriopsis* spp., *Tortunema* spp., *Rugosoopsis* spp.) are common in Proterozoic successions.

In the taxonomic section and in the figure legends, taxa are identified by: Slide number -England Finder coordinates.

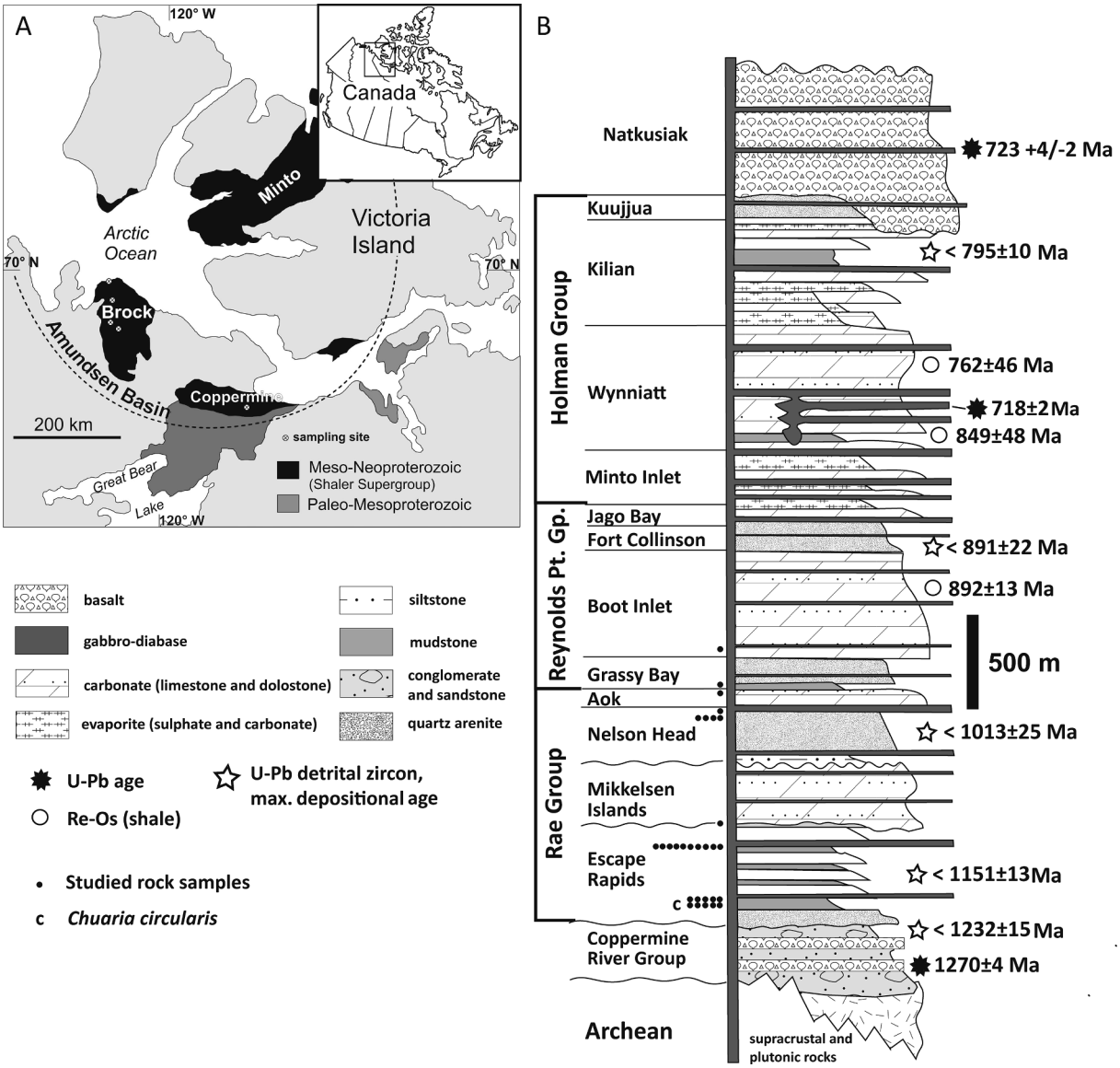

Fig. 1. A) Location of study area in northwestern Canada highlighting inliers of late Mesoproterozoic-Neoproterozoic rocks of the Shaler Supergroup. B) Generalized stratigraphic column for the Shaler Supergroup, modified from Rainbird et al. (2018), with approximate location of the sampled strata and numbers of samples collected from each U-Pb geochronology of mafic intrusions from Heaman et al., 1992; Macdonald et al., 2010 and Lecheminant and Heaman, 1989. U-Pb detrital zircon geochronology from Rainbird et al., 2018 and Rayner and Rainbird, 2013. Re-Os geochronology from van Acken et al., (2013).

4. Microfossils diversity of the lower Shaler Supergroup

Sixty-three taxa were recovered from the 26 fossiliferous samples (Table 1). Eukaryotes were recorded in the Grassy Bay, Nelson Head and Escape Rapids formations, with at least 18, 15, and 6 distinct identified taxa, respectively. The highest taxonomic diversity of other taxa (*incertae sedis* and filamentous forms) is also found in those assemblages (22 in Grassy Bay Fm.; 31 in Nelson Head Fm.; and 28 in Escape Rapids Fm.). From the assemblages of Boot Inlet, Aok and Mikkelsen Island formations, 3, 7, and 1 ambiguous taxon are reported, respectively. No eukaryotes were recovered from those formations.

4.1. Unornamented taxa

Microfossils that exhibit a simple morphology with no conspicuous ornamentation dominate the assemblages. Spheroidal smooth-walled vesicles of *Leiosphaeridia* ranging from tens to hundreds of micrometers in diameters are present in all fossiliferous samples with the exception of one sample from Boot Inlet (15RAT-T16). Jankauskas et al. (1989); Butterfield et al. (1994) and Hoffman and Jackson (1994) have divided the genus into artificial size-class species based on the size frequency distribution and the thickness of their wall (commonly based on color, opacity or fold morphology). However, the color may vary depending of the original composition of the wall, the taphonomy or the thermal maturity (not to mention the setting of microscopic light, imaging and human eye) (see discussion in Butterfield et al, 1994; Javaux and Knoll, 2016) and some microfossils interpreted as *Leiosphaeridia crassa* (with diagnostic "thick" wall) may have, in fact, thinner wall than some specimens of *L. minutissima* (with "thin" wall), as demonstrated by ultrastructural studies of specimens from the Roper Group (Javaux et al., 2003; 2004). Javaux and Knoll (2016) rather suggested that the morphology of taphonomic folds (lanceolate/sinuous) may reflect original differences in wall flexibility and therefore constitute a more relevant identification criterion than wall thickness (difficult to assess without ultra-thin section) or color to sort those microfossils into morphospecies. The size-class species established is more disputable since population statistics do not show a clear cut at 70 µm (Grey, 1999; Javaux and Knoll, 2016) but keeping this classification and adding the

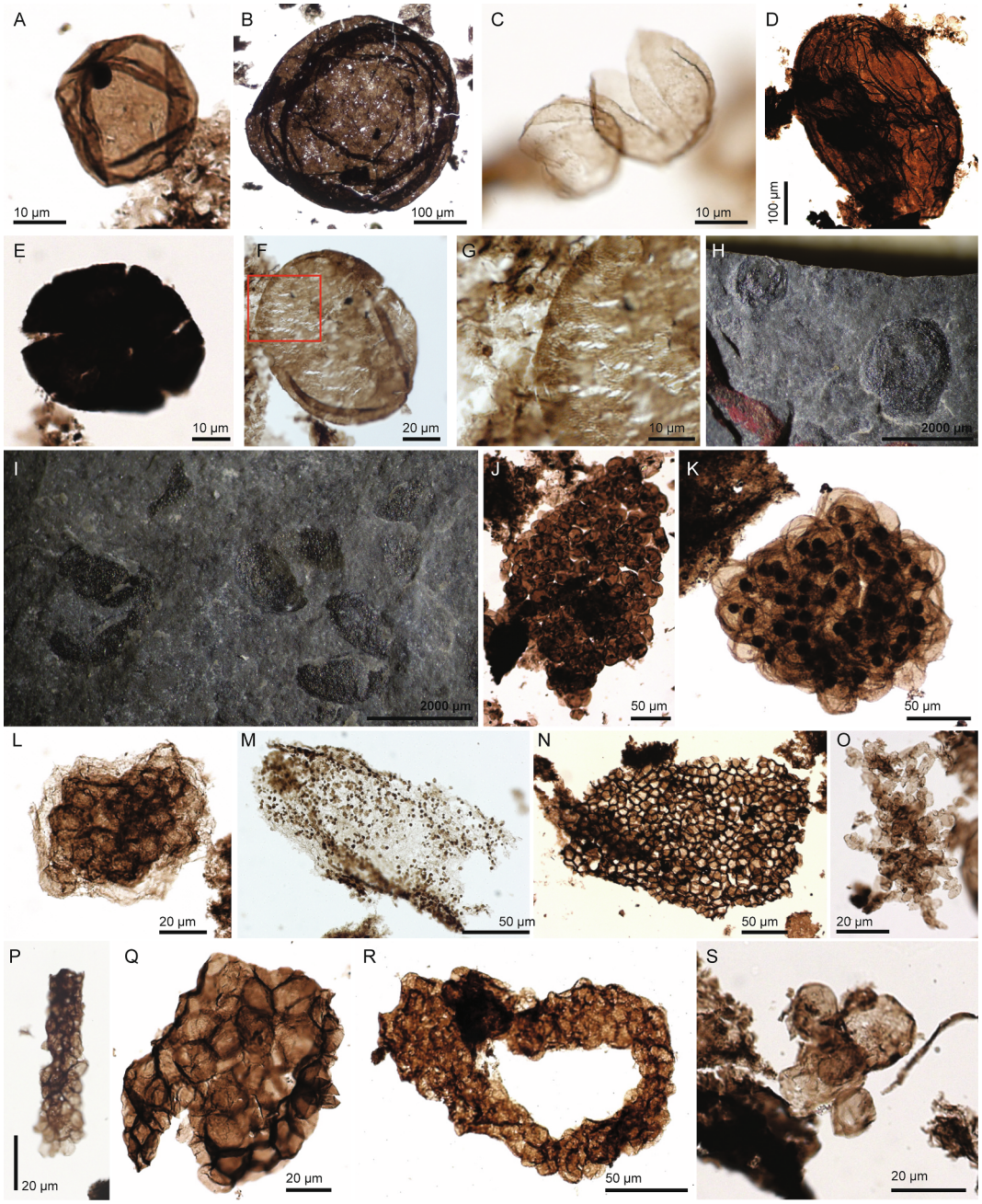

Fig. 2. *Incertae sedis.* (A) *Leiosphaeridia crassa,* 74641-Q40; 15RAT-021A1. (B) *L. jacutica,* 76139-H54; CP15-DD007 140,5m. (C) *L. minutissima* opening through medial split, 74705-C30,3; 15RAT-T17. (D) *L. tenuissima*, 74655-K52 ; 15RAT-T17. (E) *L. ternata,* 74640-O53 ; 15RAT-021A1. (F) Unnamed spheromorph with stretched striated surface texture, 75309-P49,4; 15RAT-021A1. (G) Detail of box in (F). (H) Macro-compression of *Chuaria circularis;* R37A1. (I) Macro-compression of *C. circularis* opening through medial split; R37A1. (J) *Symplassosphaeridium sp.*, 74640-S39,4; 15RAT-021A1. (K) *Synsphaeridium* sp., 75330-N50; 15RAT-T17. (L) *Myxococcoides minor,* 75330-P38 ; 15RAT-T17. (M) *Gyalosphaera* sp., 75330-U46,4 ; 15RAT-T17. (N) *Ostiana microcystis,* 73843-N54 ; 14RATB5-3A. (O) *Eosynechococcus moorei,* 74639-G57 ; 15RAT-021A1. (P) *Chlorogloeaopsis contexta,* 76141-S57 ; 15RAT-021A1. (Q – R) *Squamosphaera colonialica,* (Q) 74655-O52 ; 15RAT-T17 ; (R) 74640-N37,3 ; 15RAT-021A1. (S) *Coneosphaera* sp., 74641-W52; 15RAT-021A1.

morphology of taphonomic folds rather than wall color constitutes a practical and less subjective way to document populations of unornamented smooth-walled microfossils within an assemblage and to compare with other assemblages worldwide. Following this principle, 5 morphospecies of *Leiosphaeridia* are identified in the lower Shaler Supergroup *L. crassa* (Naumova, 1949) Jankauskas *in* Jankauskas et al., 1989 (< 70 µm with lanceolate folds; Fig. 2A); *L. jacutica* (Timofeev, 1966) Jankauskas et al., 1989 (> 70 µm, with lanceolate folds; Fig. 2B); *L. minutissima* (Naumova, 1949) Jankauskas et al., 1989 (< 70 µm, with thin sinuous folds; Fig. 2C); *L. tenuissima* Eisenack, 1958 (> 70 µm, with thin sinuous folds; Fig. 2D); and *L. ternata* (Timofeev, 1966) Jankauskas et al., 1989 (opaque vesicle with radial breakage; Fig. 2E). As mentioned above, this classification is informal and these species are probably polyphyletic (and different developmental stages), as suggested by differences in multilayered and unilayered wall ultrastructures analyzed only in a few assemblages (Javaux et al, 2004; Moczydłowska and Willman, 2009; Willman, 2009), and may include both prokaryotes and eukaryotes.

The Grassy Bay and Nelson Head formations also contain spheroidal and subspheroidal vesicles that exhibit a stretched and diffuse striated surface texture (unnamed spheromorph; Fig. 2F, G). Although they show similar characteristics in the two formations, it is also possible

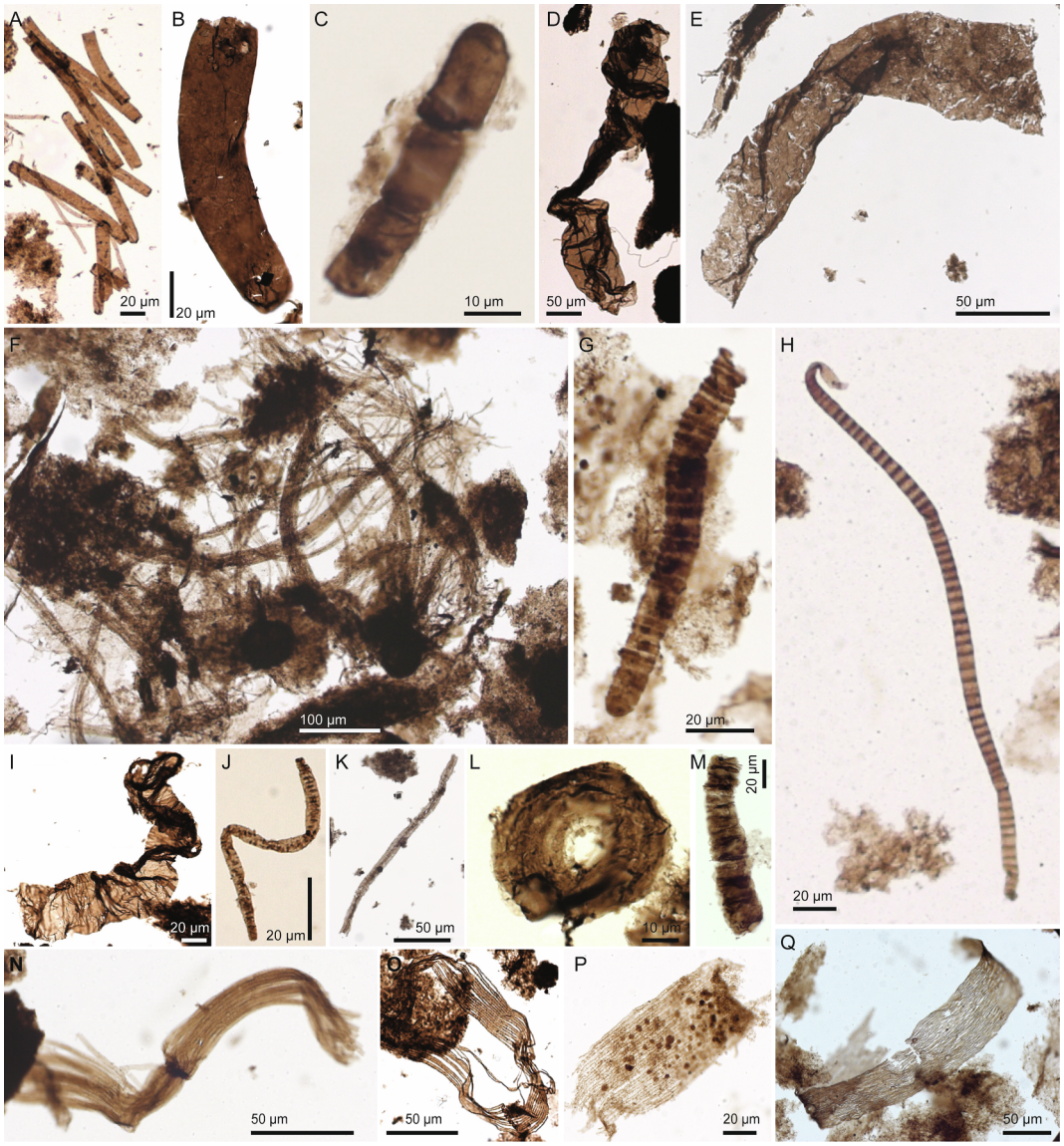

Fig. 3. *Incertae sedis* and filamentous forms. (A) *Navifusa bacillaris*, 74636-S48,3; 15RAT-T17. (B) *N. majensis*, 74640-Y43; 15RAT-021A1. (C) *Arctacellularia tetragonala*, 75333-G31; 15RAT-021A1. (D) *Syphonophycus gigas*, 75330-R50,1; 15RAT-T17. (E) *S. punctatum*, 74640-P53,1; 15RAT-021A1. (F) Mat of *Syphonophycus typicum, S. robustum* and *Polythrichoides lineatus*, 74706-T37; 15RAT-T17. (G) *Oscillatoriopsis amadeus,* 75568-T51,2; 15RAT-T17. (H) *Tortunema wernadskii,* 75564-V31,4; 15RAT-T17. (I) *Rugosoopsis latus*, 75335-J45,4; 14RATAI-516A1. (J) *Palaeolyngbya catenata,* 75330-Q56,2; 15RAT-T17. (K) *Eoschyzothrix composita* sp., 76139-C56,3; CP15-DD007 140,5m. (L) *Obruchevella valdaica*, 74710-U36; 15RAT-021A1 (M) *Eosolena* sp., 73840-Q32,2; 14RATAI_0IIA1 B. (N) *Polythrichoides lineatus*, 75329-X34; 15RAT-T17. (O – Q) Unnamed filament ; (O) 74636-T45 ; 15RAT-T17. (P) 75565-E39,3 ; 15RAT-T17. (Q) 74656-U32,2 ; 15RAT-T17.

that they represent taphonomic variants of *Leiosphaeridia* or *Valeria* (see Section 7).

The surfaces of shale samples from the lower Escape Rapids Formation (no. CP15-DD007 140.5 m; R37A1) show macroscopic specimens of large, spheroidal, opaque vesicles interpreted as *Chuaria circularis* (Walcott, 1899) Vidal and Ford, 1985 (600 – 2400 µm; n = 20; Fig. 2H, I).

Another characteristic of the lower Shaler Supergroup assemblages is the abundance of colonial and clustered vesicles. These microfossils are simple and are commonly referred to by their genus name only. Taxa present include clusters of loosely aggregated vesicles (*Symplassosphaeridium* spp.; Fig. 2J); closely aggregated vesicles (*Synsphaeridium* spp.; Fig. 2K); clusters of spheroids embedded in an external matrix (*Myxoccoides minor* Schopf, 1968 (Fig. 2L); colonies of small cells of *Gyalosphaera* sp. (Fig. 2M; see in section 7); monostromatic colonies of *Ostiana microcystis* Hermann *in* Timofeev et al., 1976 (Fig. 2N)); and small colonies of bacilliform cells (*Eosynochococcus moorei* Hofmann, 1976; Fig. 2O). Filamentous colonies with rows of packed, 3 to 5 µm spheroidal cells with no external sheath are identified as *Chlorogloeaopsis contexta* (Hermann, 1974) Hofmann and Jackson, 1994 (Fig. 2P). The Grassy Bay, Nelson Head and Escape Rapids formations yield irregularly shaped, smooth-walled *Squamosphaera colonialica* (Jankauskas, 1979) Tang *in* Tang et al., 2015 (Fig. 2Q, R), with prominent bulges on their wall surface interpreted as imprints left on the wall by unpreserved interior cells (for discussion of the genus, see Tang et al., 2015; Javaux and Knoll, 2016; Porter and Riedman, 2016;). The morphology of *S. colonialica* suggests a prokaryotic affinity rather than eukaryotic, because it resembles pleurocapsalean cyanobacteria (Javaux and Knoll, 2016). Throughout the succession, specimens of *Coneosphaera* sp. consisting of a large central spheroid with attached smaller spheroids of more or less uniform size are present (Fig. 2S).

The assemblages from the Grassy Bay and Nelson Head formations contain the netromorph microfossils *Navifusa bacillaris* (Herman, 1981) Hoffman and Jackson, 1994 (Fig. 3A)), and elongated specimens of *N.*

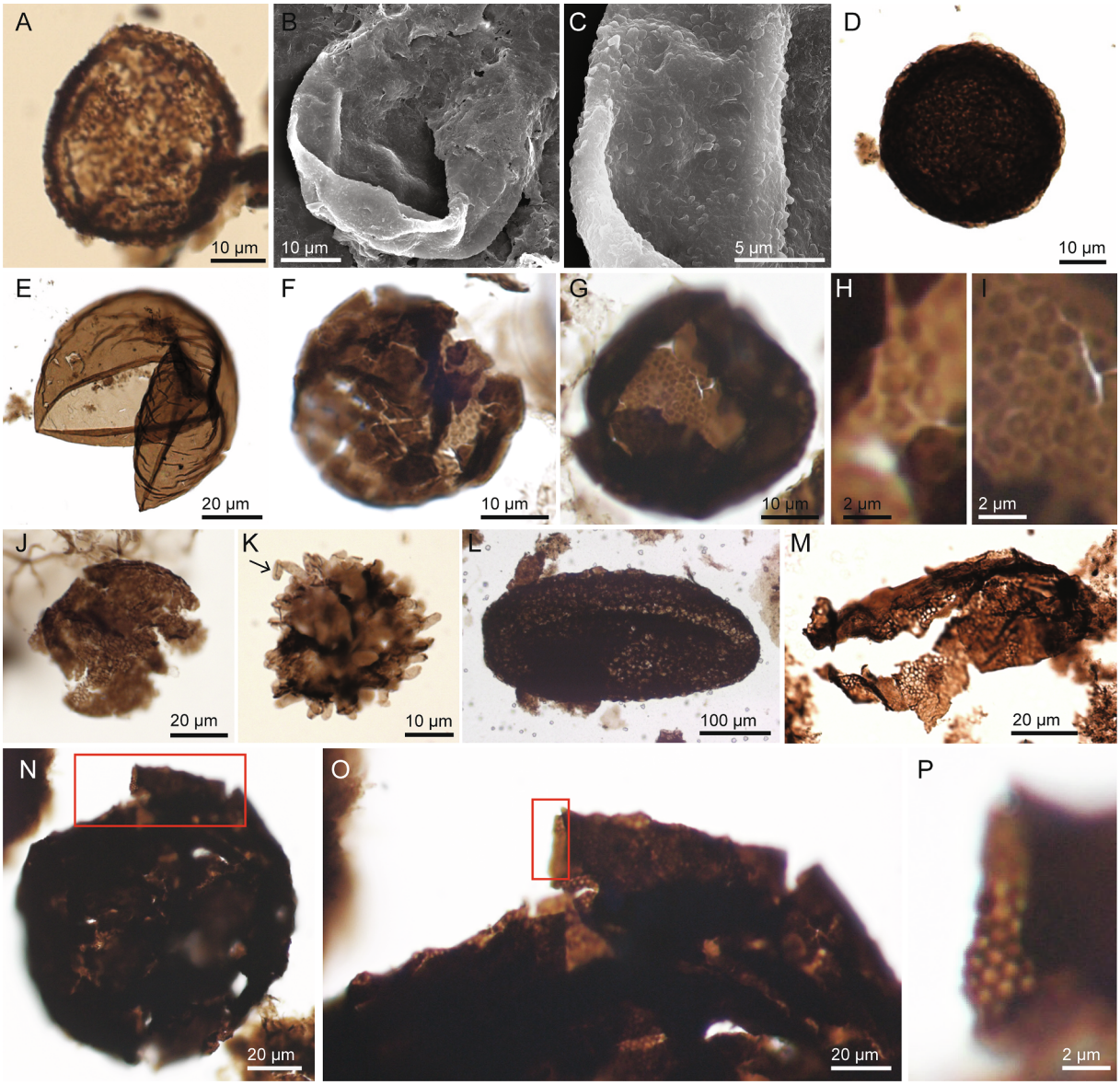

Fig. 4. Eukaryotes. (A – C) *Vidalopalla verrucata* ; (A) 74714-N29,1 ; 15RAT-021A1 ; (B – C) SEM pictures, lame 5, 15RAT021A1. (D) *Culcitulisphaera revelata*, 74636-P39,4; 15RAT-T17 ; 15RAT-T17. (E) *Valeria lophostriata* opening through medial split 75330-H52-2; 15RAT-T17. (F – I) *Nunatsiaquus cryptotorus* n. gen., n. sp.; (F, H) 74641-G44,1; 15RAT-021A1. (G, I) Holotype, 74641-L34; 15RAT-021A1. (J) *C. foveolatus*, 74713-H28; 15RAT-021A1. (K) *Microlepidopalla mira*, 74641-C52,2 ; 15RAT-021A1. (L) *M.* sp., 74,637 ; 15RAT-T17. (M) *Dictyosphaera macroreticulata*, 73843-O29,2; 14RATB5-3A. (N – P) *D. tacita*, 75309-F50,3; 15RAT-021A1. (O) Detail of box in (N). (P) Detail of box in (O).

majensis Pyatiletov, 1980 (Fig. 3B). In addition, small chains of barrel-shaped vesicles of *Arctacellularia tetragonala* (Maithy, 1975) Hofmann and Jackson, 1994 are rare, but present in the Grassy Bay Formation (Fig. 3C).

4.2. Filamentous taxa

Filamentous microfossils are abundant throughout the lower Shaler Supergroup. Specimens of *Siphonophycus* (Schopf, 1968) Knoll, Swett and Mark, 1991 (individual unseptate filamentous sheaths, isolated or in bundle) are present, along with trichomes (septate filaments with or without external sheath, isolated or in bundle) and fragments of filamentous microbial mats. Filamentous sheaths were arbitrarily sorted into eight size-class species based on width by Maithy (1975), Butterfield et al. (1994) and Tang et al. (2013). Specimens belonging to seven of those species are present: *S. septatum* (Schopf, 1968) Knoll, Swett and Mark, 1991 (1– < 2 µm); *S. robustum* (Schopf, 1968) Knoll, Swett and Mark, 1991 (2– < 4 µm) (Fig. 3F); *S. typicum* (Hermann, 1974) Butterfield *in* Butterfield et al., 1994 (4– < 8 µm) (Fig. 3F); *S. kestron* Schopf, 1968 (8– < 16 µm); *S. solidum* (Golub, 1979) Butterfield et al., 1994 (16– < 32 µm); *S. punctatum* Maithy, 1975 (32– < 64 µm) (Fig. 3E) and *S. gigas* Tang *in* Tang et al., 2013 (64–128 µm) (Fig. 3D). These groupings do not reflect biological affinity, and may represent different taxa or, alternatively, growth variants within a few species but, as for *Leiospheridia*, this constitutes a useful taxonomic tool to catalogue filaments and to describe the diversity of morphospecies and compare to other assemblages' diversity and paleoecology, even if they may not correspond to the true biological diversity, a problem well known by paleontologists. The same principle was used for trichomes of uniseriate cells *Oscillatoriopsis* (Schopf 1968) Butterfield et al., 1994, pseudoseptate filaments of *Tortunema* (Hermann, 1974) Butterfield et al., 1994, and transversely wrinkled smooth filaments of *Rugosoopsis* (Timofeev and Hermann, 1979) Butterfield et al., 1994. The present material contains: *O. obtusa* Schopf 1968 (3 – 8 µm wide) and *O.*

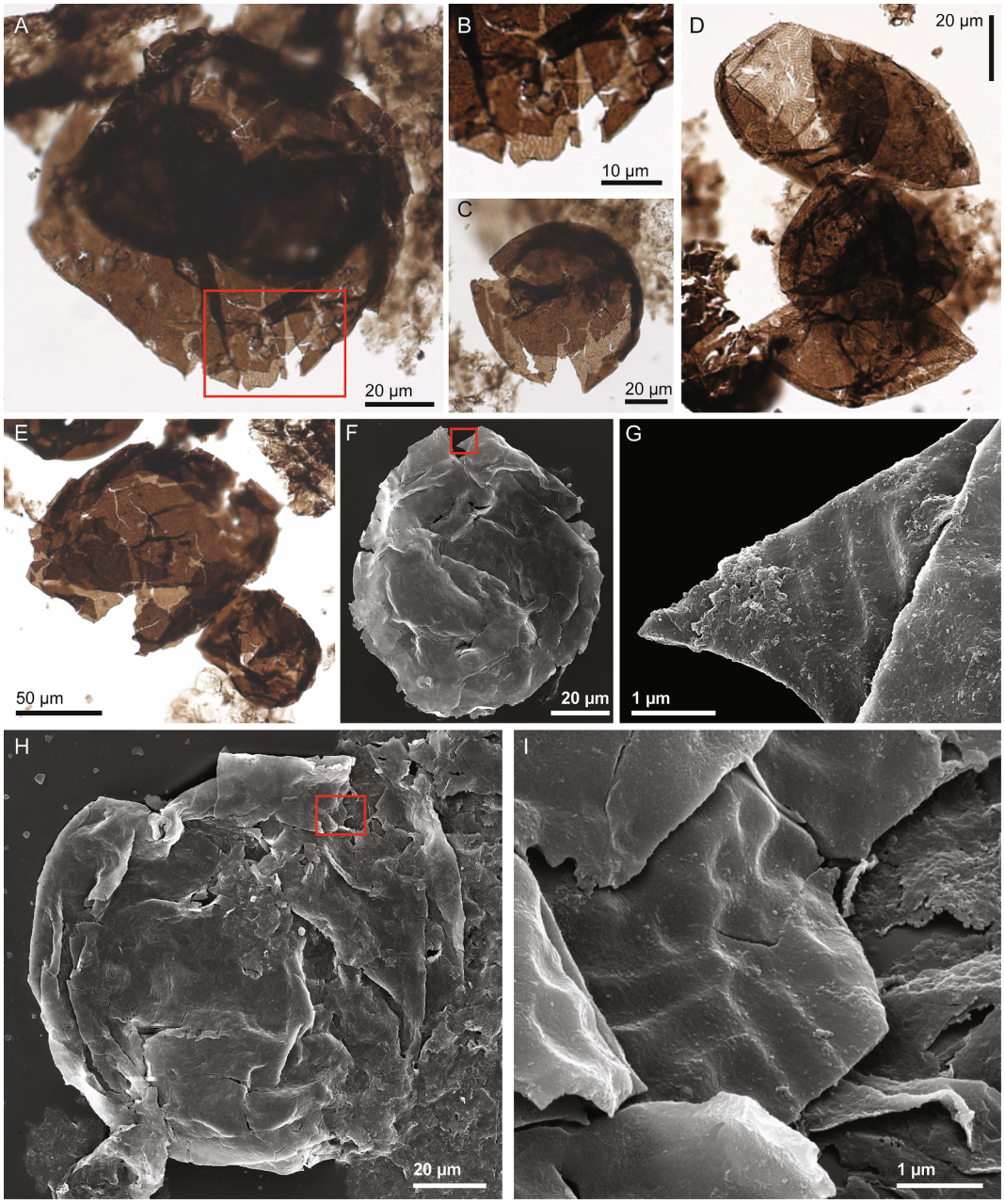

Fig. 5. *Daedalosphaera digitisigna* n. gen., n. sp. (A) Holotype; possibly smaller vesicles enclosed in the main vesicle; 74640-F52,3. (B) Detail of box in (A) showing ornamentation. (C) 74640-Y34,2. (D) 74639-E27,4; opening through medial split. (E) 74640-G37,4. (F – I) SEM pictures, lame 3. (G) and (I) Detail of boxes in (F) and (H), respectively, showing the ornamentation on the inner wall surface. All specimens from 15RAT-021A1.

amadeus (Schopf and Blacic, 1971) Butterfield et al., 1994 (8 – 14 µm wide) (Fig. 3G); *T. angusta* Kolosov, 1984 (< 10 µm) and *T. wernadskii* (Shepeleva, 1960) Butterfield et al., 1994 (10 – 25 µm) (Fig. 3H); and *Rugosoopsis tenuis* Timofeev and Hermann, 1979 (> 50 µm) and *R. latus* Pyatiletov, 1980 (> 50 µm) (Fig. 3I).

Other filamentous species present include *Palaeolyngbya catenata* Hermann, 1974, an unbranched, uniseriate individual trichome enclosed by a smooth-walled sheath, 8 – 16 µm wide (Butterfield et al., 1994) (Fig. 3J); *Eoschizothrix composita* Seong-Joo and Golubic, 1998, a filamentous sheath enclosed in another filamentous sheath (Fig. 3K); and *Obruchevella valdaica* (Shepeleva, 1974) Jankauskas et al., 1989, a compressed, non-septate, concentrically arranged tubular filament (Fig. 3L). Filaments of *Obruchevella* are morphologically simple, and several genera have been successively erected for similar spiromorph morphotypes. However, these are probably congeneric with *Obruchevella,* the senior taxon (see Hoffman and Jackson, 1994; and Baludikay et al, 2016, for discussion). Compressed tubular filaments with thick, regularly distributed cross-ribs of *Eosolena* sp. are present in the Escape Rapids Formation, but the specimens are considerably narrower (~20 – 30 µm; n = 4; Fig. 3M) than the other species of *Eosolena* Hermann and Timofeev, 1985 (*E. loculosa* Hermann and Timofeev, 1985 (200 – 800 µm), *E. anisocyta* Hermann and Timofeev, 1985 (450 – 750 µm) and *E. minuta* Vorob'eva *in* Vorob'eva et al., 2015 (110 – 190 µm). The specimens recovered from the lower Shaler Supergroup are left under open nomenclature because their simple morphology and the paucity of specimens plead no need for the establishment of a new species.

Finally, tight bundles of smooth-walled, unbranched filaments *Polythrichoides lineatus* (Hermann, 1974) Hermann, 1974 (Fig. 3F, N), and planar associations of parallel filaments linked by a thin organic

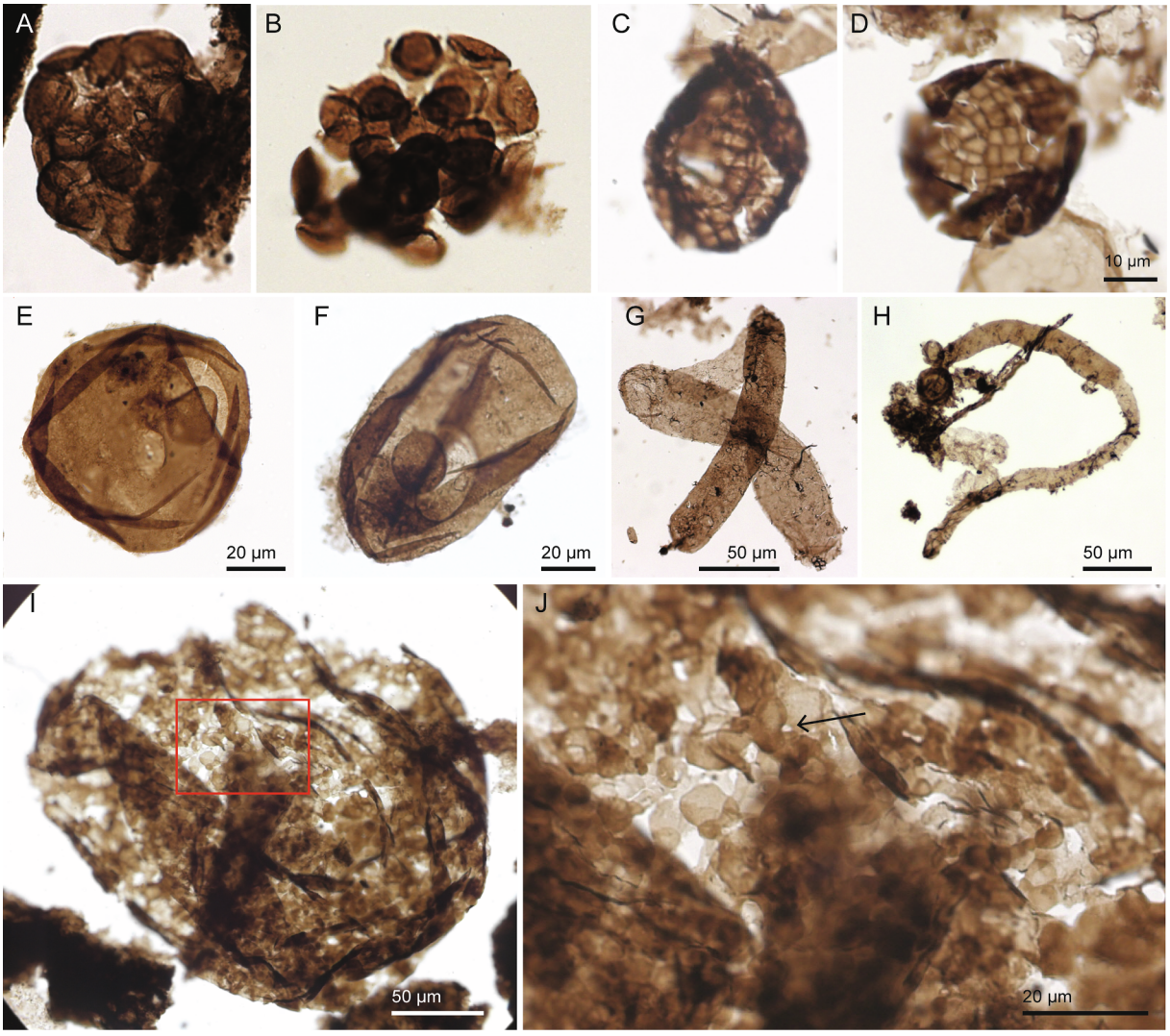

Fig. 6. Eukaryotes. (A – D) *Satka favosa* ; (A) 75330-L34,1 ; 15RAT-T17 ; (B) 74638-P52 ; 15RAT-T17 ; (C) 74641-R42,1 ; 15RAT-021A1; (D) 74641-L32; 15RAT-021A1. (E – F) *Leiosphaeridia kulgunica*; (E) 75565-G57,4; 15RAT-T17; (F) 75491-M49 ; 15RAT-T17. (G – H) *Jacutianema solubila*; (G) 74639-H57; 15RAT-021A1; (H) 74657-H53,1; 15RAT-021A1. (I – J) *Palaeastrum* sp., 74656-S48,3; 15RAT-T17. (J) Detail of box in (I), the arrow shows tripartite connection.

matrix (unnamed filament; Fig. 3O–Q) are present. The original diagnosis for the genus *Polythrichoides* (Hermann, 1974) Hermann, 1974 refers only to bundles of trichomes (Timofeev et al., 1976; see translated diagnosis in Sergeev et al., 2012) and does not fit with the morphology of the unnamed filaments reported here.

All such filamentous taxa are usually interpreted as being prokaryotic, possibly cyanobacteria (Butterfield et al., 1994), but larger specimens of *Siphonophycus* (*S. septatum* and *S. gigas*) may, alternatively, represent remains of filamentous eukaryotes (Beghin et al., 2017a). However, size alone is not a reliable criterion for determining biological affinities (Javaux et al., 2003).

4.3. Eukaryotes

At least twenty-five taxa from the present assemblages are recognized as eukaryotes, based on morphological traits characteristic of eukaryotes (Table 2) (Javaux et al., 2001, 2003, 2004), such as conspicuous surface ornamentation of a recalcitrant wall, wall structure and ultrastructure, presence of processes, complex excystment features (pylome), and multicellular organization with complex attachment among cells (Butterfield, 2009), a combination of characters unknown in prokaryotes.

Ornamented taxa show conspicuous surface ornamentation such as thick verrucae (*Vidalopalla verrucata* (Vidal and Siedlecka, 1983) Riedman and Porter, 2016; Fig. 4A – C), cushion-like outpockets (*Culcitulisphaera revelata* Riedman and Porter, 2016; Fig. 4D), concentric striations (*Valeria lophostriata* (Jankauskas, 1979) Jankauskas, 1982; Fig. 4E) and tomaculate depressions (*Caelatimurus foveolatus* Riedman and Porter, 2016; Fig. 4J). The ornamentation may be located on the inner wall surface, like the randomly distributed ridges of *Daedalosphera digitisigna* n. gen., n. sp. (Fig. 5) and the toroidal depressions in *Nunatsiaquus cryptotorus* n. gen., n. sp. (Fig. 4F – I), and consequently, are visible only when vesicles are broken.

Vesicles of *Microlepidopalla mira* Porter and Riedman, 2016 (Fig. 4K), and *M.* sp. (Fig. 4L) display a surface ornamentation made of scale-like ellipsoids. In *Microlepidopalla* sp., these ellipsoids are characteristic, but the vesicles are considerably larger (150 – 210 × 255 – 435 µm (n = 6); ellipsoids: 5 – 15 × 7.5 – 17.5 µm) than those of the type species, *M. mira* (32.5– 43.4 µm vesicles and 2.5–5 × 3.3–7.5 µm ellipsoids; n = 6).

Three taxa possess a wall made of tessellated hexagonal platelets (*Dictyosphaera macroreticulata* Xing and Liu, 1973 (Fig. 4M); *D. tacita* Tang et al., 2015 (Fig. 4N – P) or polygonal plates (*Satka favosa*; Fig. 6A – D)). Agić et al. (2015) synonymized all existing species of *Dictyosphaera* under *D. macroreticulata*, the type species. Shortly after, Tang et al. (2015) erected the new species *D. tacita* from the Tonian Gouhou

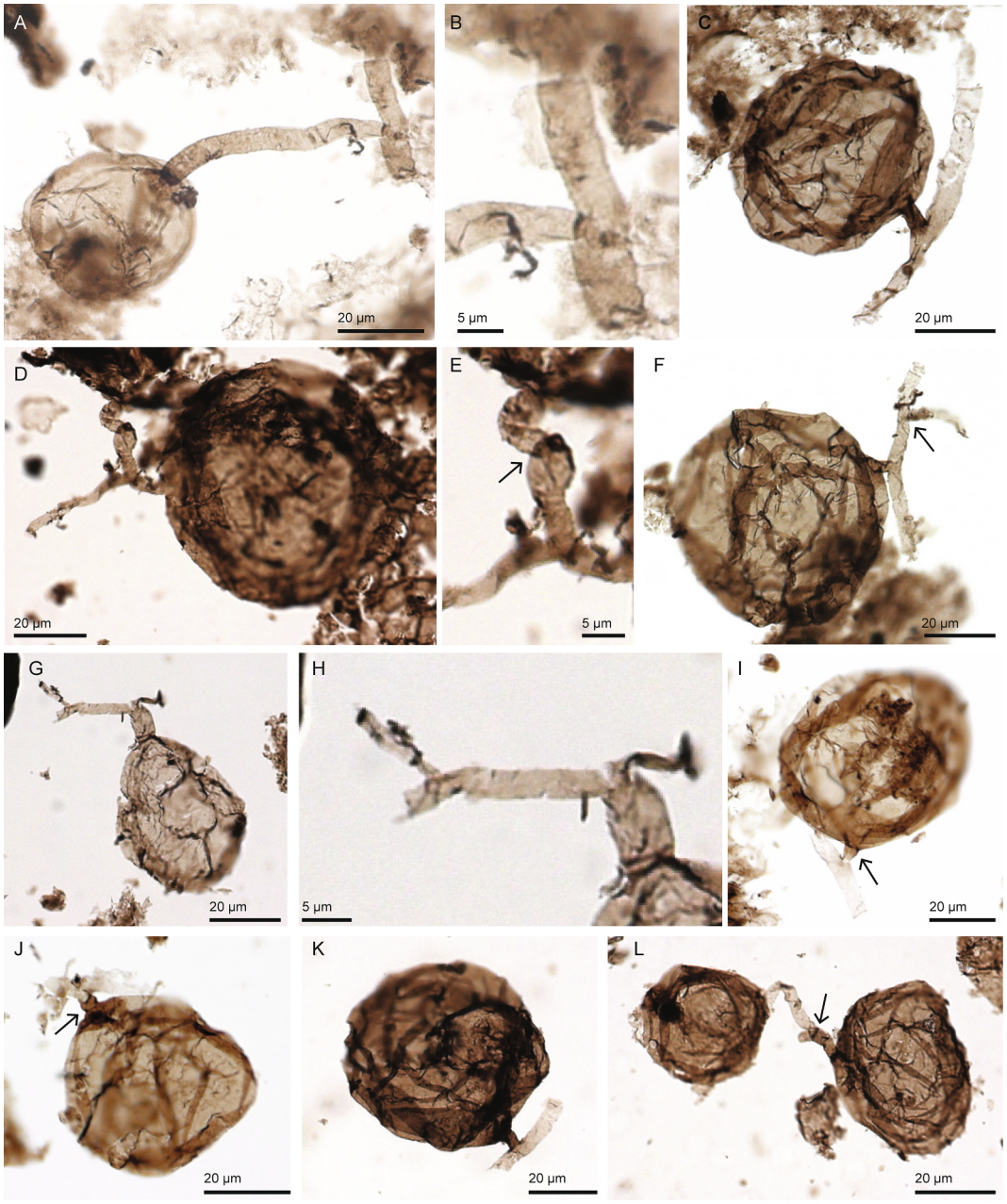

Fig. 7. *Ourasphaira giraldae* new genus, new species. (A) Holotype; 74639-W46,3. (B) Detail from (A) showing the process branching. (C) 74710-Q52,2. (D) 74639-Q43,1. (E) Detail of from (D). (F) 75309-G49,2. (G) Paratype; 74640-G29,2. (H) Detail of the process of (G) showing second and third order branching and septa between segments. (I) 74639-M30. (J) 74639-L27. (K) 74639-Z30. (L) Vesicles connecting through their processes; 74641-T31,4. Arrows in (E) and (F) show second and third order branching of the process; arrows in (I) and (J) show bulbous protrusions of the process base; arrow in (L) shows septate connection between processes. All specimens from 15RAT-021A1.

Formation in China and differentiated it from *D. macroreticulata* by the presence of smaller platelets located only on the interior of the vesicle (< 0.9 µm in *D. tacita* and 1 – 6 µm in *D. macroreticulata*). In the lower Shaler Supergroup, 3 specimens of *Dictyosphaera* recovered from the Grassy Bay Formation fit the description of *D. tacita.* It is possible *D. tacita* constitutes a junior synonym of *D. macroreticulata* or belongs to a genus distinct from *Dictyosphaera* (see section 7) but the rarity of *D. tacita* in the lower Shaler Supergroup prevents a meaningful taxonomic revision.

The circular opening of the smooth-walled *Leiosphaeria kulgunica* Jankauskas et al., 1989 (Fig. 6E, F), is interpreted as a pylome, an excystment structure that opens to liberate the cyst content. Jankauskas et al. (1989) referred to an operculum, but none were present in their material. In other reports of *L. kulgunica,* the operculum is also absent (Beghin et al., 2017a). In the present material, the operculum is present in all specimens, but has commonly fallen inside the vesicle. Porter and Riedman (2016) described the species *Kaibabia gemmulella* as having a verrucate operculum and identified *L. kulgunica* as a possible synonym of this species. The record of the smooth-walled operculum for each specimen in the present material permits to reject this synonymy and to maintain valid *L. kulgunica*, the senior taxon.

A multicellular organization, with complex attachment between cells is documented in three taxa from the lower Shaler Supergroup: various morphotypes of the filamentous taxon *Jacutianema solubila* (Timofeev and Hermann, 1979) Butterfield, 2004 (Fig. 6G, H),; colonies of cells with prominent attachment structures *Palaeastrum* sp. (Fig. 4I, J); and *Ourasphaira giraldae* n. gen., n. sp. with individual septate and branching processes (Fig. 7). The multicellularity documented here is

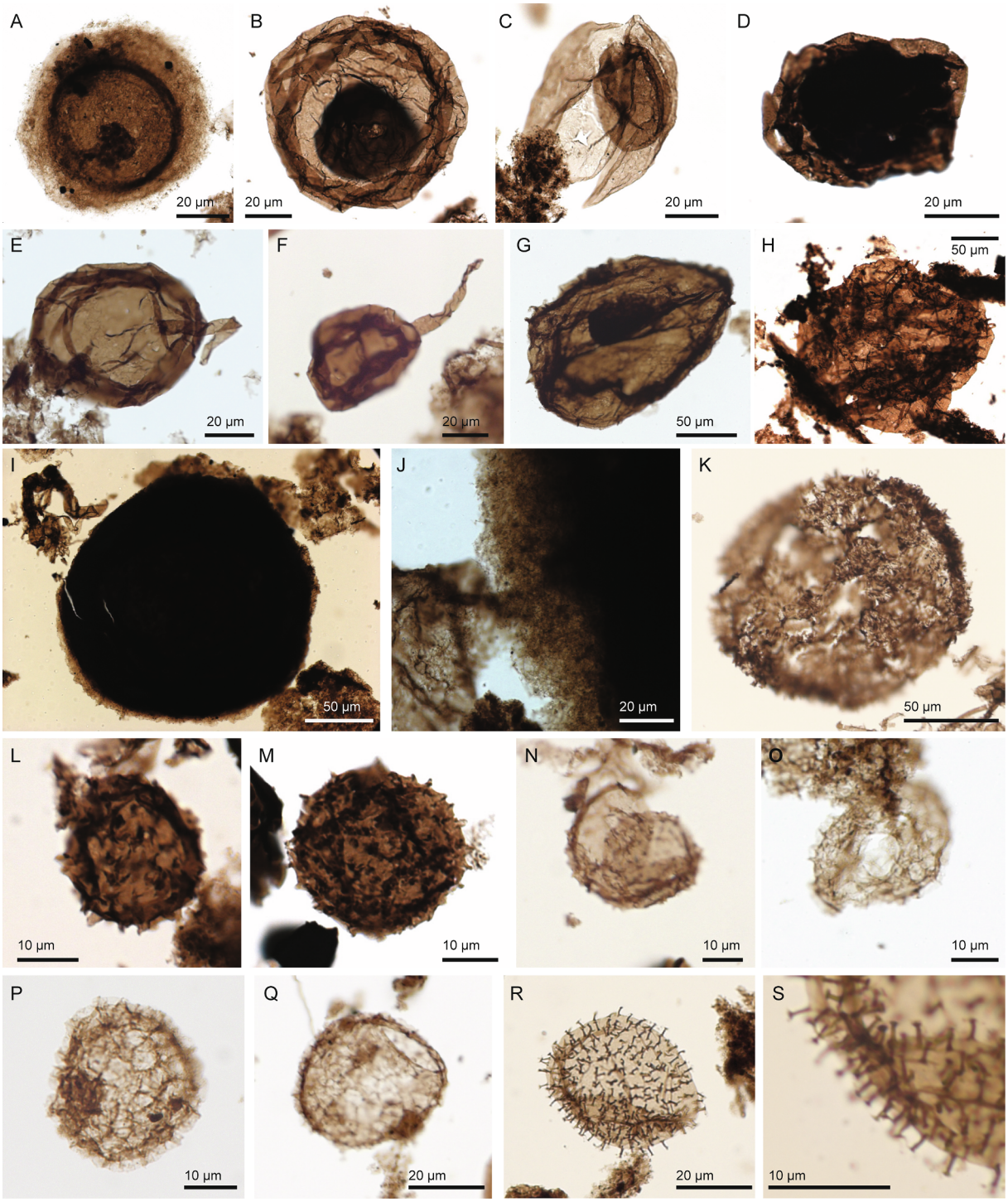

Fig. 8. Eukaryotes. (A) *Simia annulare*, 75330-J55,1; 15RAT-T17. (B – C) *Pterospermopsimorpha insolita*; (B) 74640-V35,3; 15RAT-021A1; (C) Opening through medial split, 75330-Y26; 15RAT-T17. (D) *P. pileiformis*, 74641-C43; 15RAT-021A1. (E – F) *Germinosphaera bispinosa*; (E) 74639-F41,4; 15RAT-021A1; (F) 74713-C50; 15RAT-021A1. (G – H) *Trachyhystrichosphaera aimika*; (G) 75564-S40,4; 15RAT-T17; (H) 73810-U51,1; 14RATAI-516A1. (I – J) *Gigantosphaeridium fibratum*; (I) 75565-Q52; 15RAT-T17. (J) showing detail of the fibrillary processes, 75565-R48; 15RAT-T17. (K) *'Comasphaeridium' tonium*, 75333-L51; 15RAT-021A1. (L – N) *Ericiosphaera triangula* n. gen, n. species; (L) Holotype; 74641-U40,4; 15RAT-021A1. (M) 74641-G45; 15RAT-021A1. (N) Opening through medial split, 74714-E56; 15RAT-021A1. (O – Q) *E. arbovela* n. gen, n. species; (O) Holotype with excystment structure (pylome); 74638-N52,3; 15RAT-T17. (P) 75568-G53,3; 15RAT-T17. (Q) with pylome; 75568-B42,3; 15RAT-T17. (R – S) Unnamed acanthomorph; (R) 75568-P46,4; 15RAT-T17. (S) detail of the processes.

more complex than the simple clonal division of prokaryotes and suggests a higher control over cellular development resulting in more highly ordered morphologies (Butterfield, 2009).

Other taxa such as *Simia annulare* (Timofeev, 1969) Jankauskas et al., 1989, with an equatorial flange (Fig. 8A), or vesicles enclosing another vesicle *Pterospermopsimorpha insolita* (Timofeev, 1969) Jankauskas et al., 1989 (smooth outer vesicle wall; Fig. 8B, C) or *P. pileiformis* (Timofeev, 1966) Jankauskas et al., 1989 (corrugated outer vesicle wall; Fig. 8D) exhibit a comparatively simple organization but are recognized as eukaryotic by many authors (e.g. Tappan 1980; Moczydłowska 2008; 2016; Moczydłowska et al., 2011; Baludikay et al., 2016; Javaux and Knoll, 2016; Agić et al., 2017; Beghin et al.,

Table 1
Microfossil distribution in the lower Shaler Supergroup. 1 = single specimen recovered; R = rare (2–15 specimens recovered); C = common (16–30 specimens recovered); A = abundant (> 30 specimens recovered).

Species →																	
Stratigraphic unit	Sample	*Caelatimurus foveolatus*	*'Comasphaeridium' tonium*	*Culcitulisphaera revelata*	*Daedalosphaera digitisigna* n.gen, n.sp.	*Dictyosphaera macroreticulata*	*Dictyosphaera tacita*	*Germinosphaera bispinosa*	*Gigantosphaeridium fibratum*	*Herisphaera arbovelata* n.gen., n.sp.	*H. triangula* n.gen, n.sp.	*Jacutianema solubila*	*Leiosphaeridia kulgunica*	*Microlepidopalla mira*	*Microlepidopalla* sp.	*Nunatsiaquus cryptotorus* n.gen, n. sp.	*Ourasphaira giraldae* n.gen, n.sp
Boot Inlet	15RAT-T16																
Grassy Bay	15RAT-021A1	R		R	A	R	R	A			A	A	R	C		R	A
Aok	15RAT-15																
Nelson Head	15RAT-T17	R		A					R	A			R	R	R		
	15RAT-02 unit 10																
	15RAT-02 unit 14																
	15RAT-02 unit 16																
	15RAT-02 unit 18												R				
Mikkelsen Island	15RAT-T27																
Escape Rapids (upper)	14 BR 15																
	14 BR 14																
	14 BR 91																
	14 BR 93																
	14 BR 95																
	14RATAI_0IIA1 A																
	14RATAI_0IIA1 B																
	13RAT-02																
	14RATAI-516A1					R											
	14RATB5-3A																
Escape Rapids (lower)	15RAT-ER3																
	15RAT-ER4					R											
	15RAT-ER5																
	08RAT-14B																
	R34A1																
	R36A1																
	R37A1											1					
	CP15-DD007 140,5m							R									
	CP15-DD007 207,2m					1		R									
	T133A1																

Species →											*Incertae Sedis* (Unornamented and colonial vesicles)					
Stratigraphic unit	Sample	*Palaeastrum* sp.	*Pterospermopsimorpha insolita*	*P. pileiformis*	*Sakta favosa*	*Simia annulare*	*Trachyhystrichosphaera aimika*	*Valeria lophostriata*	*Vidalopalla verrucata*	Unnamed Acanthomorph	*Arctacellularia tetragonala*	*Chloroglocaeopsis contexta*	*Chuaria circularis*	*Coneosphaera* sp.	*Gyalosphaera* sp.	*Eosolena* sp.
Boot Inlet	15RAT-T16															
Grassy Bay	15RAT-021A1		C	A	R		R	R	R		R			C		
Aok	15RAT-15															
Nelson Head	15RAT-T17	R	R		R	C	R	C	R	1				R	R	
	15RAT-02 unit 10															

(*continued on next page*)

Table 1 (*continued*)

Species →											*Incertae Sedis* (Unornamented and colonial vesicles)					
Stratigraphic unit	Sample	*Palaeastrum* sp.	*Pterospermopsimorpha insolita*	*P. pileiformis*	*Sakta favosa*	*Simia annulare*	*Trachyhystrichosphaera aimika*	*Valeria lophostriata*	*Vidalopalla verrucata*	Unnamed Acanthomorph	*Arctacellularia tetragonala*	*Chlorogloeaopsis contexta*	*Chuaria circularis*	*Coneosphaera* sp.	*Gyalosphaera* sp.	*Eosolena* sp.
	15RAT-02 unit 14						R							R		
	15RAT-02 unit 16							R								
	15RAT-02 unit 18							R								
Mikkelsen Island	15RAT-T27															
Escape Rapids (upper)	14 BR 15															
	14 BR 14															
	14 BR 91															
	14 BR 93		R													
	14 BR 95															
	14RATAI_0IIA1 A						R									
	14RATAI_0IIA1 B						C									R
	13RAT-02															
	14RATAI-516A1						C							R		R
	14RATB5-3A						C									R
Escape Rapids (lower)	15RAT-ER3		R				R									
	15RAT-ER4		R				R									
	15RAT-ER5															
	08RAT-14B															
	R34A1															
	R36A1															
	R37A1					R						R	C			
	CP15-DD007 140,5m		R										C			
	CP15-DD007 207,2m		R			R	R					R				
	T133A1															

Species →		*Incertae Sedis* (Unornamented and colonial vesicles)														Filamentous forms
Stratigraphic unit	Sample	*Eosynochococcus moorei*	*Leiosphaeridia crassa*	*L. tenuissima*	*L. minutissima*	*L. jacutica*	*L. ternata*	*Myxococcoides minor*	*N. bacillaris*	*N. majensis*	*Ostiana microcystis*	*Squamosphaera colonialica*	*Symplassiosphaeridium* spp.	*Synsphaeridium* spp.	Unnamed Sphaeromorph	*Eoschizothrix composita*
Boot Inlet	15RAT-T16															
Grassy Bay	15RAT-021A1	R	A	C	C	C	R	R		R	R	C	C	A	R	
Aok	15RAT-15		A		C	C	R							C		
Nelson Head	15RAT-T17	R	A	C	C	C		R	C		R	C		C	R	
	15RAT-02 unit 10		R													
	15RAT-02 unit 14				C		R		R							
	15RAT-02 unit 16		R													
	15RAT-02 unit 18		C		C									A		
Mikkelsen Island	15RAT-T27		R													

(*continued on next page*)

Table 1 (*continued*)

Species →		*Incertae Sedis* (Unornamented and colonial vesicles)														Filamentous forms
Stratigraphic unit	Sample	*Eosynochococcus moorei*	*Leiosphaeridia crassa*	*L. tenuissima*	*L. minutissima*	*L. jacutica*	*L. ternata*	*Myxococcoides minor*	*N. bacillaris*	*N. majensis*	*Ostiana microcystis*	*Squamosphaera colonialica*	*Symplassiosphaeridium* spp.	*Synsphaeridium* spp.	Unnamed Sphaeromorph	*Eoschizothrix composita*
Escape Rapids (upper)	14 BR 15															
	14 BR 14															
	14 BR 91		R		R											
	14 BR 93		C													
	14 BR 95															
	14RATAI_0IIA1 A		C		C											
	14RATAI_0IIA1 B	R	C		C						R			C		
	13RAT-02															
	14RATAI-516A1	R	C		R	R					R			C		
	14RATB5-3A		R	R	C						R		R			
Escape Rapids (lower)	15RAT-ER3		A	C	A	C						R				
	15RAT-ER4		C											C		
	15RAT-ER5															
	08RAT-14B		C													
	R34A1		R			R										
	R36A1		R													
	R37A1		A	C	A	C	R					R		C		
	CP15-DD007 140,5m		A	C	A	C						C		A		A
	CP15-DD007 207,2m		A	C	A	R					R	C		C		R
	T133A1		R			R								R		

Species →		Filamentous forms														
Stratigraphic unit	Sample	*Obruchevella valdaica*	*Oscillatoriopsis amadeus*	*O. obtusa*	*Palaeolyngbya catenata*	*Polythrichoides lineatus*	*Rugosoopsis tenuis*	*R. latus*	*Siphonophycus septatum (1- < 2 μm)*	*S. robustum (2- < 4 μm)*	*S. typicum (4- < 8 μm)*	*S. kestron (8- < 16 μm)*	*S. solidum (16- < 32 μm)*	*S. punctatum (32– < 6-4 μm)*	*S. gigas (64–12-8 μm)*	*Tortunema angusta*-T. wernadski Unnamed Filament
Boot Inlet	15RAT-T16									A	A	C				
Grassy Bay	15RAT-021A1	R				R	R			R	C	C	R			
Aok	15RAT-15									A	A		R			
Nelson Head	15RAT-T17	R	R	R	C	C	C	R	R	C	A	A	C	R	R	RC R
	15RAT-02 unit 10															
	15RAT-02 unit 14										R					
	15RAT-02 unit 16															
	15RAT-02 unit 18	R			R				R	R	C					
Mikkelsen Island	15RAT-T27															

(*continued on next page*)

Table 1 (*continued*)

Species →		Filamentous forms														
Stratigraphic unit	Sample	*Obruchevella valdaica*	*Oscillatoriopsis amadeus*	*O. obtusa*	*Palaeolyngbya catenata*	*Polythrichoides lineatus*	*Rugosoopsis tenuis*	*R. latus*	*Siphonophycus septatum (1- < 2 μm)*	*S. robustum (2- < 4 μm)*	*S. typicum (4- < 8 μm)*	*S. kestron (8- < 16 μm)*	*S. solidum (16- < 32 μm)*	*S. punctatum (32– < 6-4 μm)*	*S. gigas (64–12-8 μm)*	*Tortunema angusta*-T. wernadski Unnamed Filament
Escape Rapids (upper)	14 BR 15															
	14 BR 14															
	14 BR 91															
	14 BR 93										R					R
	14 BR 95															
	14RATAI_0IIA1 A										C					RR
	14RATAI_0IIA1 B				R	R	R	R			C					
	13RAT-02									R	R					RR
	14RATAI-516A1						R	R		C	C	R				
	14RATB5-3A	R														R
Escape Rapids (lower)	15RAT-ER3															
	15RAT-ER4	R														
	15RAT-ER5															
	08RAT-14B	R								R	R					
	R34A1															
	R36A1															
	R37A1	A								C	C			R		R
	CP15-DD007 140,5m					R				C	A	R	R			
	CP15-DD007 207,2m					R				R						
	T133A1	R									R					

1 = a single specimen recovered
R = rare; 2–15 specimens recovered
C = common, 16–30 specimens recovered
A = abundant, > 30 specimens recovered

Table 2
Microfossil features characteristic of eukaryotic affinity and time range.

Species	Vesicle in a vesicle/ Double wall	Surface ornamentation / Tesselated plates	excystment: medial split	excystment: pylome	Irregularly arranged processes	Regularly arranged processes	Multicellular	Indicative size range	Time Range
Caelatimurus foveolatus		X						27–53.3 μm (N = 9)	early Mesoproterozoic-late Tonian
'Comasphaeridium' tonium						X		55–130 μm (N = 3); processes 2–7 μm (n = 7)	late Mesoproterozoic - Neoproterozoic
Culcitulisphaera revelata		X						30.9–66.9 μm (N = 13)	late Mesoproterozoic-late Tonian
Dictyosphaera macroreticulata		X						37.2–109.5 μm (N = 10)	early Mesoproterozoic-early Neoproterozoic (Grassy Bay Fm, this study)
Dictyosphaera tacita		X						45–103,3 μm (N = 3)	early Neoproterozoic
Daedalosphaera digitisigna n. gen., n. sp.	X	X	X					46.3–144.2 μm (N = 40)	early Neoproterozoic (Grassy Bay Fm, this study)
Germinosphaera bispinosa			X		X			20–77.2 μm (N = 20); processes 5–57.6 μm (n = 20)	Mesoproterozoic-Neoproterozoic
Gigantosphaeridium fibratum						X		196–392.3 μm (N = 3)	early Mesoproterozoic - late Mesoproterozoic (uppermost Nelson Head Fm, this study)
Herisphaera triangula n. gen., n. sp.			X			X		21.5–32.2 μm (N = 11); processes 1.2–2.5 μm (n = 16)	early Neoproterozoic (Grassy Bay Fm, this study)
Herisphaera arbovelata n. gen., n. sp.				X		X		17.5–37.5 μm (N = 25)	late Mesoproterozoic (uppermost Nelson Head Fm, this study)
Jacutianema solubila	X						X	L = 51.5–370.8 μm; W = 15.4–41.2 μm (N = 10)	late Mesoproterozoic-early Neoproterozoic
Leiosphaeridia kulgunica				X				43.4–73.3 (N = 7); operculum 14.2–19.8 μm (n = 7)	late mesoproterozoic-early Neoproterozoic
Microlepidopalla mira		X						32.5–43.4 × 54–65 μm (N = 6); ellipsoids: 2.5–5 × 3.3–7.5 μm (n = 8)	early Neoproterozoic (Grassy Bay Fm, this study) -Mid-Neoproterozoic (late Tonian)
Microlepidopalla sp.		X						150–210 × 255–435 μm (N = 4); ellipsoids 5–15 × 7.5–17.5 μm (n = 6)	late Mesoproterozoic (uppermost Nelson Head Fm, this study)
Nunatsiaquus cryptotorus n. gen, n. sp.		X						28.4–37,5 μm (N = 8)	early Neoproterozoic (Grassy Bay Fm, this study)
Ourasphaira giraldae n. gen., n. sp.					X		X	33.1–80 μm (N = 27); processes 10–35 μm (n = 25)	early Neoproterozoic (Grassy Bay Fm, this study)
Palaeastrum diptocranum							X	216.6–347.6 μm (N = 3); Cells 5–11.6 μm (n = 8)	Mesoproterozoic-mid Neoproterozoic
Pterospermopsimorpha insolita	X		X					39.3–72.1 μm (N = 14); inner cell 15.45–61.8 μm (n = 14)	Paleoproterozoic-Neoproterozoic
Pterospermopsimorpha pileiformis	X		X					24.7–61.8 μm (N = 28); inner cell 16.5–42 μm (n = 28)	Mesoproterozoic-early Neoproterozoic
Sakta favosa		X						27–48.9 μm (N = 5)	early Mesoproterozoic-early Neoproterozoic (Grassy Bay Fm, this study)
Simia annulare		X						46.3–351.4 μm (N = 12)	Mesoproterozoic-Neoproterozoic
Trachyhystrichosphaera aimika					X			72.1–92.5 μm (N = 13)	late Mesoproterozoic-early Neoproterozoic (pre-Cryogenian)
Valeria lophostriata		X	X					75–314.15 (N = 8)	Paleoproterozoic-Neoproterozoic
Vidalopalla verrucata		X						27.5–43.3 μm (N = 3)	early Neoproterozoic
Unnamed Acanthomorph						X		37.8 μm (N = 1); processes 2.5–2.8 μm (n = 7)	late Mesoproterozoic (uppermost Nelson Head Fm, this study)
Unnamed Sphaeromorph		X?						74.8–79.5 × 90.5–115 μm (N = 10)	late Mesoproterozoic (uppermost Nelson Head Fm, this study) - early Neoproterozoic (Grassy Bay Fm, this study)

2017a; Loron and Moczydłowska, 2017).

Vesicles bearing processes are remarkably diverse in the lower Shaler Supergroup. Vesicles of *Germinosphaera bispinosa* (Mikhailova, 1986) Butterfield et al., 1994 (Fig. 8E, F), with individual unbranched processes, are present in the Grassy Bay, Nelson Head and lower Escape Rapids formations. These formations also contain many specimens of *Trachyhystrichosphaera aimika* (Hermann, 1974) Butterfield et al., 1994 (Fig. 8G, H), vesicles with variable morphology (tomaculate to spheroidal) and size, and bearing numerous, small, randomly distributed heteromorphic tubular processes.

Several taxa are characterized by evenly distributed processes around the vesicle. Large opaque vesicles of *Gigantosphaeridium fibratum* Agić et al., 2015 (Fig., 8I, J) with thin fibrillar processes are present in the Nelson Head Formation. The processes are densely arranged and < 0.5 μm wide, and are therefore visible only at high magnification. In the Grassy Bay Formation, a few specimens exhibit short, solid, simple, thin processes and a large size (Fig. 8K), and are similar to the '*Comasphaeridium' tonium* Zhang, 1995 described from the ca. 750 Ma Alinya Formation, Australia (fig. 4.2 – 4.4 in Riedman and Porter, 2016; fig. 24A – G in Zhang, 1995). However, Riedman and Porter (2016) considered the generic assignment to the Mesozoic genus *Comasphaeridium* to be dubious. The specimens from this study resemble those of Riedman and Porter (2016) and Zhang (1995), but differ from other contemporaneous examples (Beghin et al., 2017a). We agree with Riedman and Porter (2016) that this would need taxonomic revision. However, the current microfossils fit the broad description of the genus given by Staplin et al (1965) ("spherical to ellipsoidal, sometimes of large size with densely crowded, thin, solid, usually simple, more or less flexible hair-like spines") and the number of specimens is not sufficient to revise it or erect a new genus. Therefore, the present microfossils are identified as '*Comasphaeridium' tonium* but the generic assignment is placed between quotation marks.

Small specimens of *Herisphaera triangula* n. gen., n. sp. (Fig. 8L–N) and *H. arbovela* n. gen., n. sp. (Fig. 8O–Q) are a significant component of the assemblages from the Grassy Bay and Nelson Head formations, respectively. *H. arbovela* resembles specimens described as "thin-walled acanthomorph with blunt processes" in Butterfield and Rainbird, 1998 (Fig. 3.I). *E. triangula* are similar to "unnamed acritarch sp. B" in Riedman and Porter, 2016 (fig. 4.5) and resemble specimens of *Goniosphaeridium* sp. in Butterfield et al., 1994 (fig. 14.F – G). However, the small number of specimens recovered by these authors makes positive synonymy difficult. Likewise, the individual specimen of unnamed acanthomorph (Fig. 8R, S) is similar to specimens of *Galerosphaera walcottii* (Vidal and Ford, 1985) Porter and Riedman, 2016, notably by the presence of funnel-shaped processes, but it is not embedded in an envelope. The paucity of specimens in the present material prevents any further recognition.

Many taxa recognized as eukaryotes and recorded in the lower Shaler Supergroup share several characteristic features (Table 2). For example, process-bearing *H. arbovela* also exhibits a pylome excystment structure (Fig. 8O, Q), and the ornamented vesicle of *D. digitisigna* may enclose other vesicles and open through a medial split (Fig. 5A, D). Such openings are also indicative that they were cysts (resistant reproductive structure) and not vegetative stages.

5. Discussion

5.1. Comparison with contemporaneous assemblages

The Wynniatt Formation in the upper Shaler Supergroup was previously investigated for paleontology (Fig. 1; Hofmann and Rainbird, 1994; Butterfield and Rainbird, 1998; Butterfield, 2005a, b). These studies revealed an important diversity of organic-walled microfossils, including acanthomorphs resembling the new genus *Herisphaera* (see section 7) and macroscopic carbonaceous compressions of *Chuaria circularis*, *Tawuia dalensis* Hofmann and Aitken, 1979, and *Beltina danai* Walcott, 1899, preserved on the bedding planes of shale samples.

Table 3 presents a comparison of the lower Shaler Supergroup assemblages with those of eight other late Mesoproterozoic – early Neoproterozoic successions. The lower Shaler Supergroup assemblage shows the greatest similarity with assemblages from the 1065–1008 Ma Mbuji-Mayi Supergroup, DRC (Baludikay et al., 2016; François et al, 2017; in review) and the 1105 ± 37 Ma Atar/El Mreïti Group, Mauritania (Beghin et al., 2017a) (22–23 common taxa). It shares also common Proterozoic taxa with other contemporaneous assemblages (9 to 16 taxa). However, the total taxonomic diversity is unprecedented for this time period, with a total of 63 taxa including 25 taxa of eukaryotes, compared to other assemblages with 22 to 39 taxa, including 3 to 11 eukaryotes. Although some of the eukaryotic taxa such as *Trachyhystrichosphaera, Valeria, Simia*, *Pterospermopsimorpha* or *Jacutianema* are commonly found in other assemblages of the same age, the lower Shaler Supergroup also records numerous new eukaryotes (see Table 3).

In the Torridon Group, Scotland (Strother et al., 2011; Battison and Brasier, 2012; Strother and Wellman, 2016), many specimens are unnamed or have been named with alternative taxonomy because of their interpreted terrestrial depositional environments (but see Stüeken et al., 2017 for a different geological interpretation). In the Torridon Group, the presence of taxa otherwise occurring in marine successions, such as *Leiosphaeridia ternata, Pterospermopsimorpha,* and an unnamed species with "circular pits" interpreted as different from *Dictyosphaera* by Strother et al, 2011, but with polygonal structures resembling *Dictyosphaera* by Javaux (pers. obs., 2008, in Javaux and Knoll, 2016, p8), also questions the non-marine interpretation of the succession. Loron and Moczydłowska (2017) suggests that the strata recording *L. ternata* represent marine ingressions. The presence of identical taxa in the Torridon Supergroup, in the Grassy Bay Formation, deposited in an estuarine environment, and other marine assemblages, suggest that marine taxa may have lingered after marine transgressions into brackish, freshwater, or terrestrial basins. Conversely, the presence of new taxa in the lower Shaler Group, might reflect exceptional preservation of taxa yet to be discovered in other marine successions, provincialism, or transport from terrestrial to marine settings through delta or estuaries. These hypotheses would require more data from unambiguous terrestrial assemblages to be tested.

However, paleontological taxonomy is usually based on morphology and those taxa may constitute junior synonyms of their respective other occurrences. For instance, *Eohalothece lacustrina* are similar to *Eosynochococcus* present in the lower Shaler Supergroup and specimens of *Trematoligotriletum* resemble the present specimens of *Vidalopalla.* Similarly, the microfossils with reticulate wall occurring in the Torridon Group are similar to specimens of *D. tacita.* In addition, some taxa reported in Strother et al. (2011) are not illustrated, making difficult comparisons between assemblages (e.g. cf. *Satka* sp.).

Taxa found worldwide in marine basins indicate free connections between them and a similar marine ecology. Differences in contemporaneous assemblages, on the other hand, may be linked to variable redox conditions or paleoecological settings (Beghin et al., 2017a,b). For example, in the Taoudeni basin, Mauritania, a high diversity of forms is preserved in proximal environments during marine transgression, probably linked to higher availability of nutrients and possibly oxygen, and proximity to estuarine environments (Beghin et al., 2017b). Similar deltaic to intertidal paleoenvironmental conditions could explain the species richness documented in the Grassy Bay and upper Nelson Head formations, but their geochemistry (paleoredox conditions and nutrients) is not yet known. The evidence of predation observed in those formations (Loron et al., 2018) could also explain the high diversity, as predation constitutes a strong selective pressure (Butterfield, 1997; Bengston, 2002; Porter, 2016; Loron et al., 2018).

Table 3
Comparison of lower Shaler Supergroup assemblages with contemporaneous assemblages. The illustrated fossils reported in the literature are compared taking into account their original and emended diagnoses. For artificial size-classes, it is only referred to the genus (*Leiosphaeridia* spp., *Syphonophycus* spp., *Tortunema* spp., *Oscilatoriopsis* spp., *Rugosoopsis* spp.) with the exception of large taxa of *Siphonophycus punctatum* and *Siphonophycus gigas*. The taxa identified as eukaryote are in bold. Taxa from other successions marked with an asterisk (*) are present in the Shaler Supergroup.

lower Shaler Supergroup (this study)	Mbuji-Mayi Supergr., DRC Baludikay et al., 2016	Atar/El Mreïti Gr., Mauritania Beghin et al., 2017a,b	lower Madhubani Gr., India Tang et al., 2017	Bylot Supergr., Canada Hofmann and Jackson, 1994	Lakhanda Gr., Russia Hermann, 1990	Liulaobei Fm., China Tang et al., 2013	Gouhou Fm. Tang et al., 2015	Mirojedikha Fm., RussiaHermann (1990)	Torridon Gr., Scotland Strother and Wellman, 2016; Strother et al., 2011
~1230–892 Ma	~1100-850	1105 ± 37	1100-720	1092 ± 59	1025 ± 40	~1000-811	~1000-811	~1000-800	994 ± 48
	Arctacellularia tetragonala *	*Arctacellularia tetragonala**	*Annulusia annulata*	*Arctacellularia tetragonala* *	*Annulusia annulata*	*Eotylotopalla? grandis*	*Chuaria circularis* *	*Aimia delicata*	*Chlorogloeaopsis spp.*
Arctacellularia tetragonala	*Chlorogloeaopsis kanshiensis*	*Chlorogloeaopsis contexta* *	***Caudosphaera expansa***	*Chlorogloeaopsis contexta* *	***Caudosphaera expansa***	*Fabiformis baffinensis*	***Dictyosphaera tacita****	*Arctacellularia tetragonala* *	cf. *Eliasum*
Caelatimurus foveolatus	*Chlorogloeaopsis zairensis*	*Chlorogloeaopsis kanshiensis*	***Devisphaera corallis***	*Chlorogloeaopsis kanshiensis*	*Elatera unistriata*	*Leiosphaeridia spp.**	*Eosynochococcus moorei* *	*Chlorogloeaopsis contexta* *	*Eohalothece lacustrina (*?)*
Chlorogloeaopsis contexta	*Coneosphaera sp.* *	*Chlorogloeaopsis zairensis*	***Jacutianema Solubila****	*Coneosphaera arctica*	*Elatera binata*	*Myxococcoides ovata*	*Fabiformis baffinensis*	*Coneosphaera sp.* *	***Germinosphaera bispinosa****
Chuaria circularis	*Eomicrocystis elegans*	*Chuaria circularis* *	*Leiosphaeridia spp.* *	*Coneosphaera sp.* *	***Eosaccoromyces ramosus***	*Navifusa majensis**	*Leiosphaeridia spp.**	*Cucumiforma sp.*	*Leiosphaeridia spp.* *
'Comasphaeridium' tonium	*Eomicrocystis malgica*	***Comasphaeridium tonium***	***?Lophosphaeridium sp.***	*Eomicrocystis elegans*	*Eosolena loculosa*	*Ostiana microcystis**	*Navifusa majensis**	*Glomovertella eniseica*	*Leiosphaeridia ternata* *
Coneosphaera sp.	*Fabiformis baffinensis*	cf *Coneosphaera sp.*	*Navifusa actinomorpha*	*Eomycrocystis malgica*	*Flabelleforma compacta*	***Pololeptus rugosus***	*Polythrichoides lineatus**	*Heliconema turukhania*	***Lophosphaeridium* sp.**
Culcitulisphaera revelata	***Germinosphaera bispinosa****	*Eomicrocystis irregularis*	*Polythrichoides lineatus**	*Fabiformis baffinensis*	*Lakhandinia prolata*	*Polythrichoides lineatus**	*Siphonophycus spp.**	*Leiosphaeridia spp.**	**cf. *Satka* sp. (*?)**
***Daedalosphaera digitisigna* n. sp.**	*Glomovertella miroedikhia*	*Eomicrocystis malgica*	***Simia annulare****	*Leiosphaeridia spp.**	*Leiosphaeridia* spp. *	***Simia simica***	*Squamosphaera colonialica**	*Myxococcoides minor**	*Siphonophycus spp.* *
Dictyosphaera macroreticulata	***Jacutianema solubila****	*Gemmuloides doncookii*	*Siphonophycus spp.**	*Leiosphaeridia ternata**	*Leiosphaeridia ternata**	***Simia annulare****	*Symplassiosphaeridium spp.**	*Navifusa bacillaris**	cf. *Stictosphaeridium*
Dictyosphaera tacita	*Leiosphaeridia spp.**	***Jacutianema Solubila****	*Siphonophycus punctatum**	***Lophosphaeridium granulatum***	*Lomentunella vaginata*	*Siphonophycus spp.**	*Synsphaeridium spp.**	*Obruchevella valdaica**	*Symplassiosphaeridium spp.* *
Eoschizothrix composita	*Leiosphaeridia ternata**	*Leiosphaeridia atava*	*Siphonophycus gigas**	*Navifusa actinomorpha*	*Majasphaeridium carpogenum*	*Siphonophycus punctatum**	*Tawuia dalensis*	*Octoedryxium truncatum*	*Synsphaeridium spp.* *
Eosolena sp.	***Lophosphaeridium granulatum***	***Leiosphaeridia kulgunica****	*Synsphaeridium spp.**	*Navifusa bacillaris**	*Majasphaeridium sp.*	*Siphonophycus gigas**	***Trachyhystrichosphaera aimika****	*Oscillatoriopsis spp.**	cf. *Trachysphaeridium* sp.
Eosynochococcus moorei	*Myxococcoides minor**	*Leiosphaeridia spp.**	*Tortunema* sp. *	*Navifusa majensis**	*Mucorites ritheicus*	*Synsphaeridium sp.**	***Valeria lophostriata****	*Palaeolyngbya hebeiensis*	***Trematoligotriletum* cf. *T. emarginatum* (*?)**
Germinosphaera bispinosa	*Navifusa actinomorpha*	*Leiosphaeridia ternata**	***Trachyhystrichosphaera aimika****	*Nostocomorpha sp.*	*Mycosphaeroides caudatus*	***Trachyhystrichosphaera aimika****	Unnamed form	*Palaeolyngbya helva*	Corrugate forms
Gigantosphaeridium fibratum	*Navifusa majensis**	*Navifusa actinomorpha*	***T. botula***	*Obruchevella valdaica**	*Myxococcoides minor**	***T. botula***		*Polythrichoides lineatus**	Disphaeromorphitae
Gyalosphaera sp.	*Obruchevella valdaica**	*Navifusa majensis**	Unnamed sp. A	Opaque filaments	*Ostiana microcystis**			***Pterospermopsimorpha pileiformis****	Ellipsoidal forms
***Herisphaera triangula* n. sp.**	Opaque filaments	*Obruchevella spp.*	Unidentifiable fragment	*Oscillatoriopsis spp.**	***Palaeovaucheria clavata***			*Sibiriafilum tunicum*	Irregular saccate forms
***Herisphaera arbovelata* n. sp.**	*Ostiana microcystis**	*Ostiana microcystis**		*Palaeolyngbya sp.**	***Pterospermopsimorpha insolita****			*Siphonophycus spp.**	**Microfossils with reticulate wall (*?)**
Jacutianema solubila	*Palaeolyngbya catenata**	*Pellicularia tenera*		*Pellicularia tenera*	***P. pileiformis****			*Synsphaeridium spp.**	**Multicellular ball**
Leiosphaeridia kulgunica	*Pellicularia tenera*	*Polysphaeroides sp.*		*Polythrichoides lineatus**	*Rugosoopsis* spp. *			***Trachyhystrichosphaera aimika****	Tapered ellipsoids

(*continued on next page*)

Table 3 (*continued*)

lower Shaler Supergroup (this study)	Mbuji-Mayi Supergr., DRC Baludikay et al., 2016	Atar/El Mreïti Gr., Mauritania Beghin et al., 2017a,b	lower Madhubani Gr., India Tang et al., 2017	Bylot Supergr., Canada Hofmann and Jackson, 1994	Lakhanda Gr., Russia Hermann, 1990	Liulaobei Fm., China Tang et al., 2013	Gouhou Fm. Tang et al., 2015	Mirojedikha Fm., RussiaHermann (1990)	Torridon Gr., Scotland Strother and Wellman, 2016; Strother et al., 2011
~1230–892 Ma	~1100-850	1105 ± 37	1100-720	1092 ± 59	1025 ± 40	~1000-811	~1000-811	~1000-800	994 ± 48
Leiosphaeridia spp.	*Polysphaeroides filiformis*	*Polythrichoides lineatus* *		***Pterospermopsimorpha insolita*** *	*Segmentothallus aspergus*			*Trachytrichoides ovalis*	Trichomes
Leiosphaeridia ternata	*Polythrichoides lineatus* *	***Pterospermopsimorpha insolita*** *		***Satka favosa*** *	***Simia nerjenica***			*Veteronostocale sp.*	
Microlepidopalla mira	***Pterospermospimorpha insolita*** *	***P. pileiformis*** *		*Siphonophycus spp.* *	*Siphonophycus punctatum* *			***Vidalopalla verucata*** *	
Microlepidopalla sp.	***P. pileiformis*** *	***Simia annulare*** *		*Siphonophycus punctatum* *	*Synsphaeridium* spp. *				
Myxococcoides minor	*Spumosina rubiginosa*	*Siphonophycus spp.* *		*Spumosina rubiginosa*	*Tortunema* spp. *				
Navifusa bacillaris	*Symplassiosphaeridium spp.* *	*Siphonophycus punctatum* *		*Squamosphaera squamifera* comb. nov.	***Trachyhystrichosphaera aimika*** *				
Navifusa majensis	*Synsphaeridium spp.* *	*Siphonophycus gigas* *		*Symplassiosphaeridium spp.* *					
***Nunatsiaquus cryptorus* n. gen., n. sp.**	***cf. Tappania sp.***	***Spiromorpha segmentata***		*Synsphaeridium spp.* *					
Obruchevella valdaica	*Tortunema spp.* *	*Spumosina rubiginosa*		***Valeria lophostriata*** *					
Oscillatoriopsis spp.	***Trachyhystrichosphaera aimika*** *	*Synsphaeridium spp.* *							
Ostiana microcystis	***T. botula***	*Tortunema spp.* *							
Ourasphaira giraldae	*Trachytrichoides ovalis*	***Trachyhystrichosphaera aimika*** *							
***Palaeastrum* sp.**	*Rugosoopsis spp.* *	***T. botula***							
Palaeolyngbya catenata	*Siphonophycus spp.* *	***Valeria lophostriata*** *							
Polythrichoides lineatus	*Siphonophycus punctatum* *	***Vidalopalla sp.***							
Pterospermopsimorpha insolita	***Valeria elongata***								
Pterospermopsimorpha pileiformis	***Valeria lophostriata*** *								
Rugosoopsis spp.	**Unnamed form**								
Sakta favosa									
Simia annulare									
Siphonophycus spp.									
Siphonophycus punctatum									
Siphonophycus gigas									
Squamosphaera colonialica									
Symplassiosphaeridium spp.									
Synsphaeridium spp.									
Tortunema spp.									
Trachyhystrichosphaera aimika									
Valeria lophostriata									
Vidalopalla verrucata									

(*continued on next page*)

Table 3 (*continued*)

lower Shaler Supergroup (this study)	Mbuji-Mayi Supergr., DRC Baludikay et al., 2016	Atar/El Mreïti Gr., Mauritania Beghin et al., 2017a,b	lower Madhubani Gr., India Tang et al., 2017	Bylot Supergr., Canada Hofmann and Jackson, 1994	Lakhanda Gr., Russia Hermann, 1990	Liulaobei Fm., China Tang et al., 2013	Gouhou Fm. Tang et al., 2015	Mirojedikha Fm., RussiaHermann (1990)	Torridon Gr., Scotland Strother and Wellman, 2016; Strother et al., 2011
~1230–892 Ma	~1100-850	1105 ± 37	1100-720	1092 ± 59	1025 ± 40	~1000-811	~1000-811	~1000-800	994 ± 48
Unnamed acanthomorph									
Unnamed sphaeromorph									
Unnamed filament									
Total taxa 53	39	36	18	30	27	16	15	24	22
Total eukaryotes 25	11	11	7	4	7	5	3	3	6 (10?)
Taxa in common with the lower Shaler Supergroup	22	23	10	16	11	10	12	13	9

5.2. Biostratigraphic significance of the lower Shaler Supergroup eukaryotes

The majority of microfossils identified as eukaryotes in the lower Shaler Supergroup are long-ranging taxa. Vesicles of *Valeria* occur from the Paleoproterozoic (Peng et al., 2009) to the pre-Cryogenian Neoproterozoic (Riedman and Porter, 2016). Similarly, the microfossils *Pterospermopsimorpha*, *Germinosphaera*, and *Simia* are well known from Mesoproterozoic and Neoproterozoic assemblages (e.g., Mikhailova, 1986; Butterfield et al., 1994; Baludikay et al., 2016; Javaux and Knoll, 2016; Sergeev et al., 2016; Agić et al., 2017; Loron and Moczydłowska, 2017).

The occurrence of *Trachyhystrichosphaera aimika* in the Escape Rapids, Nelson Head, and Grassy Bay formations confirms the biostratigraphic value of the taxon as a potential index fossil for the late Mesoproterozoic to early Neoproterozoic (Butterfield et al., 1994; Tang et al., 2013; Baludikay et al., 2016).

Dictyosphaera macroreticulata is known from India, Australia, and China, and recently from the *ca.* 1.5 Ga Greyson Formation in the Belt Supergroup of Montana (Adam et al., 2017). This species is usually considered as an index taxon for Mesoproterozoic successions, commonly co-occuring with specimens of *Valeria* and *Tappania* (Agić et al., 2015, 2017; Javaux and Knoll, 2016; Adam et al., 2017). Thus, the presence of *D. macroreticulata* in the < 1013 – 892 ± 13 Ma Grassy Bay Formation confirms the presence of the taxon in Laurentia (and for the first time in Canada), and extends the species' biostratigraphic range into the early Neoproterozoic. Also, the record of *D. tacita* in the Grassy Bay Formation constitutes only the second occurrence of this taxon (first in Laurentia), in strata similar in age to the lower Gouhou Formation, China (Tang et al., 2015). The occurrence of *Dictyosphaera tacita* in the lower Shaler Supergroup, and in the Gouhou Formation (Tang et al., 2015) may also suggest a biostratigraphic role for this taxon for early Neoproterozoic strata only if future investigations report it in other areas worldwide.

Also reported here is the youngest occurrence, and first record in Laurentia, of *Gigantosphaeridium*, previously known only from the early Mesoproterozoic Ruyang Group, China (Agić et al., 2015). The record of *G. fibratum* in the < 1013 – 892 ± 13 Ma Nelson Head Formation extends the biostratigraphic range of the species to the entire Mesoproterozoic.

Other taxa are, for the first time, documented beyond their known stratigraphic range. Prior to this study, *Satka favosa* was reported exclusively from the Mesoproterozoic (Jankauskas et al., 1989; Nagovitsin, 2009; Javaux and Knoll, 2016; Adam et al., 2017; Agić et al., 2017) and vesicles of *Microlepidopalla* were only previously described from the < 782 – 751.0 ± 7.6 Ga Galeros Formation, Chuar Group, Arizona (Porter and Riedman, 2016; for age constraint see Rooney et al., 2017).

Chuaria circularis is common in Precambrian assemblages, occurring mainly in the early Neoproterozoic (Talyzina, 2000). The species is present in the < 1.23 Ga lower Escape Rapids Formation, in the ca. 0.8 Ga Wynniatt Formation (Hofmann and Rainbird, 1994) and in the correlative strata from the Mackenzie Mountains Supergroup (Hofmann, 1985) but is absent from all intervening stratigraphic units.

Another peculiarity of the lower Shaler Supergroup is the presence of small acanthomorphs with evenly scattered processes (Fig. 8). Acanthomorphs are a major constituent of the Ediacaran biota (Grey, 1999; Knoll et al., 2006; Cohen and Macdonald, 2015) but they have large diameters. Rare older occurrences of acanthomorphs with regularly distributed processes include *Shuiyousphaeridium* Yin, 1997, *Gigantosphaeridium* and *Comasphaeridium* Staplin et al., 1965 (see Beghin et al., 2017a and ref. therein) but these have also large diameters (> 50–100 μm). By contrast, small acanthomorphs (< 40 μm) with regularly distributed processes are characteristic of early Cambrian planktonic biota (see Butterfield, 1997; Bengston, 2002 and ref. therein). Thus, the presence of *Herisphaera triangula* n. sp., *H. arbovela* n. sp., and the unnamed acanthomorph identified in the present work may

suggest that such small acanthomorphs diversified earlier. However, local ecological variations and possible preservation biases may also play a role in their absence from other successions.

5.3. Implications for early eukaryotic diversification

Attempts to reconstruct Proterozoic organic-walled fossil diversity have been numerous (Knoll, 1994; Vidal and Moczydłowska-Vidal, 1997; Knoll et al., 2006; Xiao and Dong, 2006; Riedman et al., 2014, Cohen and Macdonald, 2015; Riedman and Sadler, 2017; Xiao and Tang, 2018) and all have shown a global trend of the major increase in species richness at ~800 Ma, followed by a late Tonian decrease to ~733 Ma and a new increase with the development of Ediacaran acritarchs.

Recent studies of the Ruyang Group in China (Yin et al., 2005; Agić et al., 2015; 2017) have shown that eukaryotes were more diverse than previously reported in the early Mesoproterozoic. Moreover, recent investigations of the Taoudeni basin in Mauritania (Beghin et al., 2017a,b) and the Mbuji-Mayi Supergroup in DRC (Baludikay et al., 2016), showed that eukaryotic taxa were also more diverse in the late Mesoproterozoic than previously documented by paleontological data and diversity models (Knoll, 1994; Vidal and Moczydłowska-Vidal, 1997; Huntley et al., 2006; Knoll et al., 2006; Xiao and Dong, 2006; Riedman et al., 2014, Cohen and Macdonald, 2015). The diversity of the lower Shaler Supergroup biota, with 25 eukaryotic species, including five new taxa and three unnamed forms, supports this observation.

All those lines of evidence suggest that the major diversification of eukaryotes may have been more gradual, starting in the Mesoproterozoic, and driven by the predation pressure, development of photosynthesis, biomineralization and other biological and abiotic factors (Cohen et al., 2011; Javaux, 2011; Porter, 2011, 2016; Agić et al., 2015; Butterfield 2015a, b; Knoll, 2015; Javaux and Knoll, 2016; Knoll and Lahr, 2016; Gibson et al., 2017; Javaux and Lepot, 2017; Loron et al., 2018).

6. Conclusions

Late Meso – to early Neoproterozoic lower Shaler Supergroup microfossil assemblages contain an unexpected diversity of organic-walled microfossils dominated by unornamented and filamentous taxa. In addition, more twenty-five eukaryotes are reported, an unprecedented record for this time interval. Four new genera and five new species are described, comprising two small acanthomorphs with evenly distributed processes, two ornamented sphaeroidal acritarchs, and one process-bearing multicellular taxon. Three unnamed forms are also reported.

Taxa otherwise characteristic of younger and older time intervals co-occur in the geochronologically well-constrained lower Shaler Supergroup, and with the late Meso – early Neoproterozoic index taxon *T. aimika*. The new stratigraphic ranges of *Dictyosphaera macroreticulata* and *Satka favosa* permit a refinement of the Proterozoic biostratigraphy of those fossils, until now considered as possible early Mesoproterozoic index taxa. The important eukaryotic diversity preserved in the lower Shaler Supergroup supports the hypothesis of a more gradual diversification of the Domain Eukarya, starting in the Mesoproterozoic, during the so-called “boring billion”, rather than around 800 Ma.

7. Systematic paleontology

All the material is stored in collections of the Department of Geology in the University of Liège, Belgium. The specimens are localized in the microscopic slides by: Slide number-England Finder coordinates (oriented with label of the left).

Domain EUKARYA Woese et al., 1990

Genus *Daedalosphaera* n. gen.

Type species: *Daedalosphaera digitisigna* n. sp. by monotypy

Diagnosis: as for the type species.

Etymology: In Greek mythology Daedalus, builder of the labyrinth in Crete. In reference to the random patterns of the vesicle wall sculpture.

Daedalosphaera digitisigna n. sp.

Fig. 5A – I

Etymology: From the latin “digiti”, fingers and “signa”, sign, imprint. In reference to the fingerprint-like appearance of the wall sculpture.

Holotype: Specimen 74640-F52,3, sample 15RAT-021A1, illustrated Fig. 5A.

Occurrence: Sample 15RAT-021A1; Shale of the Grassy Bay Formation in the Brock Inlier, Northwestern Territories, Canada.

Diagnosis: Vesicles circular to sub-circular in outline (originally spheroidal and sub-spheroidal) with more or less optically dense wall. The wall is smooth on its outer surface and displays a rugulate surface sculpture made of randomly distributed ridges and grooves of various lengths and constant width on its inner surface. The vesicle excysts through medial split.

Material: Hundreds of well-preserved specimens in sample 15RAT-021A1 along with numerous fragments and broken vesicles in various state of preservation.

Dimensions: The vesicles range in diameter from 46.3 to 144.2 µm. (n = 40). The ridges forming the wall sculpture vary in length but are consistently ~0.5 µm wide.

Remarks*:* The specimen illustrated in Fig. 5A seems to enclosed 2 internal vesicles with diameters of 40 and 36.6 µm but this may represent taphonomic superimposition and, therefore, is not included in the diagnostic of the species.

D. digitisigna n. sp. differs from *Volleyballia dehlerae* Porter and Riedman, 2016 by the location and pattern of the wall sculpture. In *V. dehlerae*, the wall sculpture is located on the outer surface of the vesicle wall whereas in *D. digitisigna* n. sp. it is located on the inner surface (see Fig. 5G, I). The wall sculpture of *D. digitisigna* is not organized in a pattern of parallel ridges, a feature diagnostic of *V. dehlerae*, and no outer envelope is present. Furthermore, *D. digitisigna* displays an excystment structure and possibly internal vesicles that are absent in *V. dehlerae*. The size range of the *D. digitisigna* is also considerably larger: 46.3 – 144.2 µm in diameter (25 – 45 µm for *V. dehlerae*).

Genus *Dictyosphaera* Xing & Liu, 1973

Type species: *Dictyosphaera macroreticulata* Xing & Liu, 1973

Remark: Agić et al. (2015) revised the genus *Dictyosphaera* by synonymizing all the previously described species with the senior species *D. macroreticulata*. Subsequently, Tang et al. (2015) described *D. tacita* for vesicles with a smooth external wall and smaller hexagonal plates, located on the inner vesicle surface, on the basis of 2 specimens. The authors suggested a reevaluation of the genus taxonomy. In the present material, the two species are represented. We agree that this would need reevaluation but, as only 3 specimens of *D. tacita* are reported from the present material, it is difficult to exhaustively reinterpret the taxonomy. Therefore, specimens of the lower Shaler Supergroup are recognized as *D. macroreticulata* and *D. tacita*, the two distinct valid species of the genus.

Dictyosphaera macroreticulata Xing & Liu, 1973

Fig. 4M

2015 *Dictyosphaera macroreticulata* Xing & Liu, 1973 – Agić et al., p. 32, figs 2.1 – 2.9.

2016 *Dictyosphaera macroreticulata* Xing & Liu, 1973 – Javaux & Knoll, p. 6, fig. 2.15.

2017 *Dictyosphaera macroreticulata* Xing in Xing and Liu (1973) – Agić et al., p. 108, Fig. 3A–F, 4A–C and 14G.

2017 *Dictyosphaera macroreticulata* – Adam et al., p. 388, Fig. 3A–C.

Lectotype: originally described as *Dictyosphaera sinica* Xing and Liu, 1973, from the Chuanlingguo Formation, northern China, Mesoproterozoic. Junior synonym of *D. macroreticulata* Xing and Liu, 1973, pl. 1, fig. 18 (Agić et al., 2015).

Material: Rare specimens, in various states of preservation in

15RAT-021A1, 14RATAI-516A1, 15RAT-ER4 and CP15-DD007 207.2 m.

Description: Spheroidal vesicles, 37.2 – 109.5 μm in diameter (N = 10), with wall composed of > 1.5 μm tessellate polygonal platelets. No external envelope and no excystment structure are observed.

Remark: D. *macroreticulata* is considered as a characteristic taxon of Mesoproterozoic rocks (e.g. Agić et al., 2015; 2017; Adam et al., 2017; Javaux and Knoll, 2016). Its presence in the < 1013 – 892 ± 13 Ma Grassy Bay Formation is interesting as it extends the biostratigraphic range of the taxon to the entire Mesoproterozoic – early Neoproterozoic.

Occurrences: Paleoproterozoic and Mesoproterozoic of China (Ruyang and Gaoshanhe Groups) (Xing and Liu, 1973; Agić et al., 2015; 2017), Roper Group, Australia (Javaux and Knoll, 2016), Belt Supergroup, Montana (Adam et al., 2017). Late Mesoproterozoic – early Neoproterozoic Escape Rapids and Grassy Bay formations, Shaler Supergroup, Canada (this study).

Dictyosphaera tacita Tang et al., 2015

Fig. 4N – P

? 2011 "Blunt ellipsoidal vesicle with a micro-reticulate wall" – Strother et al., p. 505, Fig. 1i, j.

2014 *Dictyosphaera* sp., Xiao et al., 2014, p. 217, Fig. 6A–B, I, J.

2015 *Dictyosphaera tacita* n. sp. – Tang et al., p. 305, fig. 10

Material: 3 well-preserved specimens in 15RAT-021A1.

Description: Optically dense spheroidal vesicles ranging from 45.0 to 109.5 μm in diameter (N = 3). The wall is made of polygonal structures < 0.8 μm is width and located on the vesicle wall inner surface.

Remarks: Specimens of *D. tacita* resemble specimens of "blunt ellipsoidal vesicle with a micro-reticulate wall" in Strother et al., 2011 (Fig. 1i, j). Javaux and Knoll (2016, p. 8) also noted their similarity with *Dictyosphaera*. Strother et al. (2011) describe their specimens as having an ornamentation made of highly-ordered pits creating a reticulate pattern. Such ornamentation seems similar to what is observed in electronic microscopy in specimens from Tang et al. (2015) (fig. 10B4). Therefore, *D. tacita* may be lacking the diagnostic tessellated polygonal platelets that made the wall of *Dictyosphaera*, and may constitute a distinct genus. Unfortunately, with no specimens available for electron microscopy, it is difficult to resolve the taxonomy using the specimens of the lower Shaler Supergroup, and these are left under the valid name *D. tacita*.

Occurrences: Tonian Gouhou Formation; China (Tang et al., 2015); Late Mesoproterozoic – early Neoproterozoic Grassy Bay formations, Shaler Supergroup, Canada (this study).

Genus *Herisphaera* n. gen.

Type species: *Herisphaera arbovela* n. sp.

Other species: Herisphaera triangula n. sp.

Diagnosis: Small spheroidal to subspheroidal vesicles bearing conical hollow processes that communicate with the vesicle interior. The processes are evenly distributed on the vesicle surface. A membrane may extend between the processes forming a reticulate pattern on the vesicle surface. Excystment mechanisms may be present.

Etymology: From latin "*her*", hedgehog and "*sphaera*", sphere. In reference to the spiny aspect of the vesicles.

Remark: The two species described here (see below), *H. triangula* and *H. arbovela*, exhibit morphological differences (presence of a membrane between the processes and of a pylome in *H. arbovela*; no membrane and opening through medial split in *H. triangula*) but both are the same size range (< 40 μm) and have small, hollow, conical processes. Therefore, the two species are described under the same genus, *Herisphaera* but as distinct species.

Small acanthomorphs are scarce prior to the Ediacaran period (Knoll et al., 2006; Cohen and Macdonald, 2015). Pre-Ediacaran process-bearing taxa include *Shuiyousphaeridium* with furcating, branching or funnel-shaped processes, *Gigantosphaeridium* with fibrillary processes, *Comasphaeridium tonium* with short, thin processes, *Tappania plana*, with irregularly distributed heteromorphic processes that may branch, may be septate, and/or with neck-like trapezoidal expansions, and *Trachyhystrichosphaera,* with irregularly distributed heteromorphic processes sometimes enveloped in a membrane. Species of *Shuiyousphaeridium*, *Gigantosphaeridium* and *Comasphaeridium* are bearing solid processes whereas species of *Herisphaera* exhibit hollow processes. Specimens of *Tappania plana* and *Trachyhystrichosphaera* may bear hollow processes but these are not evenly distributed on the vesicle as in species of *Herisphaera.*

Herisphaera arbovela n. sp.

Fig. 8O – Q

?1998 thin-walled acanthomorph with blunt processes – Butterfield, Fig. 3.I, p. 964

Etymology: From the Latin "*arbor*", mast and "*vela*", sails. In reference to the appearance of the thin organic matrix around the processes, similar to the sails on the boat's mast.

Holotype: Specimen 74638-N52,3, sample 15RAT-T17; illustrated in Fig. 8O.

Occurrence: Sample 15RAT-T17; Shale of the upper Nelson Head Formation in the Brock Inlier, Northwestern Territories, Canada.

Diagnosis: Small spheroidal to subspheroidal vesicle with psilate wall and bearing abundant sharp, hollow, conical processes that are regularly distributed on the vesicle surface. Thin membrane extends between the processes forming a reticulate pattern on the vesicle surface. Excystment through pylome.

Material: Hundreds of well-preserved specimens in sample 15RAT-T17

Dimensions: The vesicles are 17.5 to 37.5 μm in diameter (n = 25). Processes are ~2 μm long. Pylome diameter 10 to 20 μm (n = 2).

Remarks: *H. arbovela* n. sp. differs from *Vandalosphaeridium reticulatum* Vidal, 1976, by the shape of the processes, which are bi- or trifurcate in *V. reticulatum* and simple and hollow in *H. arbovela*. In *V. reticulatum*, the processes are wider and connect with each other at their bases, whereas in *E. arbovela* they have short bases and are connected only by a thin membrane at their tips. Additionally, *V. reticulatum* does not exhibit a pylome opening and is much larger than *E. arbovela* (44 – 83 μm in diameter).

Herisphaera triangula n. sp.

Fig. 8L – N

?1994 Goniosphaeridium sp. – Butterfield et al., p. 40, fig. 14.F – G.

?2016 Unnamed acritarch sp. B – Riedman and Porter, p. 877, fig 4.5.

Etymology: From the Latin "*triangula*", triangles, in reference to the shape of the processes.

Holotype: Specimen 74641-U40,4, sample 15RAT-021A1; illustrated in Fig. 8L.

Occurrence: Sample 15RAT-021A1; Shale of the Grassy Bay Formation in the Brock Inlier, Northwestern Territories, Canada.

Diagnosis: Small spheroidal to subspheroidal vesicle. The wall is psillate and bears numerous, hollow, evenly distributed conical processes, triangular in shape. Excystment through medial split.

Material: Tens of well-preserved specimens in sample 15RAT-021A1.

Dimensions: The vesicle diameter ranges from 21.5 to 32.2 μm (n = 11) whereas the processes are 1.2 – 2.5 μm long (n = 16).

Remarks*: H. triangula* resembles specimens of *Goniosphaeridium* sp. described in Butterfield et al. (1994), but one specimen has processes that possibly branch (fig. 14G in Butterfield et al., 1994), which is not observed for *E. triangula*.

The taphonomic alteration of the vesicles of *H. triangula* resulted in rolling up of some processes that are locally rod-shaped.

Genus *Nunatsiaquus* n. gen.

Type species: *Nunatsiaquus cryptotorus* n. sp. by monotypy

Diagnosis: as for the type species.

Etymology: From "*Nunatsiaq*", Inuktitut name of the Northwestern Territories in Arctic Canada, where the microfossils have been found.

Nunatsiaquus cryptotorus n. sp.

Fig. 4F – I

Etymology: From the latin "*crypticus*", hidden, and "*torus*", a tore. In reference to the shape of the wall sculptures and their location on the inside of the vesicle wall.

Holotype: Specimen number 74641-L34, sample 15RAT-021A1, illustrated in Fig. 4G, I.

Occurrence: Sample 15RAT-021A1; Shale of the Grassy Bay Formation in the Brock Inlier, Northwestern Territories, Canada.

Diagnosis: Vesicle circular in outline, originally sphaeroidal, with smooth and optically dense wall. The inner surface of the wall is sculptured with round to polygonal depressions surrounded by an elevated rim and bearing a central knob, visible only after breaking of the vesicle wall.

Material: Eight well-preserved specimens from sample 15RAT-021A1.

Dimensions: vesicles 28.4 to 37.7 μm in diameter (n = 8). The toroidal depressions are 0.8 – 1 μm in diameter (n = 20).

Remarks*: N. cryptotorus* differs from vesicles of *Dictyosphaera macroreticulata* by the location of the ornamentation on the inner wall, and the shape of the ornaments. The wall of *Dictyosphaera* is made of tessellated hexagons (Javaux et al., 2004; Agić et al., 2015), whereas the ornamentation in *N. cryptotorus* consists of doughnut-shaped depressions upon the wall inner surface. Moreover, the breaking of the vesicles indicates that the wall is not made of an assemblage of small platelets. Finally, the depressions are circular and consistently ~1 μm in diameter, differing from the hexagonal platelets of *Dictyosphaera,* which range in diameter from < 0.9 to 6 μm.

The inner ornamentation is interesting in that it reveals a diversity that is perhaps existing but overlooked in other Proterozoic assemblages. Other examples of inner wall surface sculpture are known from *Dictyosphaera tacita* (Tang et al., 2015), *Valeria lophostriata* (Javaux et al., 2004) and *Daedalosphaera digitisigna* n. gen., n. sp. (see above).

Ourasphaira n. gen.

Type species: Ourasphaira giraldae n. gen., n. sp., by monotypy

Diagnoses: as for the type species.

Etymology: From the ancient Greek "*οὐρά*" (*ourá*), tail and "σφαῖρα" (sphaîra), sphere.

Ourasphaira giraldae n. sp.

Fig. 7A – L

Etymology: Named in honor to M. Giraldo, who dedicated her professional life to the preparation of palynological samples at the University of Liege and who is retiring in 2018.

Holotype: Specimen 74639-W46,3, sample 15RAT-021A1; illustrated in Fig. 7A.

Paratype: Specimen 74640-G29,2, sample 15RAT-021A1; illustrated in Fig. 7G.

Occurrence: Sample 15RAT-021A1; Shale of the Grassy Bay Formation in the Brock Inlier, Northwestern Territories, Canada.

Diagnosis: Organic-walled spheroidal vesicles bearing a single "T"-shaped bifurcating process occasionally with second and third order branches. Branches are separated by septa or communicate freely with each other and with the vesicle. Bulbous protrusions occasionally present at the bases of processes.

Material: Hundreds of well-preserved specimens in sample 15RAT-021A1.

Dimensions: The vesicles are 33.1 to 80.0 μm in diameter (n = 27). The processes are 10 – 35 μm from their base to the extremity of the main branches.

Remarks*:* The specimen illustrated Fig. 7L shows two vesicles of the same size and same appearance, connected together by their respective processes. Septa are not universally present. Processes locally communicate freely with the interior of the vesicle (Fig. 7C, K).

Specimens of the genus *Germinosphaera* may bear single processes but they are unseptate and do not branch. Specimens of *Germinosphaera fibrilla* (Ouyang, 1974) Butterfield et al., 1994, exhibit a morphology ~~close~~ resembling *O. giraldae* (e.g. fig 17.F, Butterfield et al., 1994) but differ by having 2–4 processes. The processes in *O. giraldae* are consistently single and "T"-shaped. Processes in *Germinosphaera* do not have bulbous protrusions at their bases as in *O. giraldae* (see Fig. 7I, J).

The process connected to the *O. giraldae* vesicle display T-shaped branching. This second-order branching, and sometimes third-order branching, occurring perpendicular to the previous branching (clearly visible on Fig. 7F), implies a greater level of cellular control than simple uniaxial extension (Niklas, 2000; Butterfield, 2009). Moreover, the septa between branches - when present - imply that they represent distinct cells. These features show that *O. giraldae* was a multicellulareukaryotic microorganism.

Genus *Palaeastrum* (Butterfield et al., 1994) Porter and Riedman, 2016

Type species: Palaeastrum dyptocranum (Butterfield et al., 1994) Porter and Riedman, 2016

Palaeastrum sp.

Fig. 6I, J

Material: Rare well-preserved specimens in Nelson Head Formation (15RAT-T17)

Description: Spheroidal colonies, 216.6 to 347.6 μm in diameter (N = 3), consisting of a single layer of ~5–12 μm ellipsoidal and spheroidal cells attached together by prominent bi- or tripartite structures.

Remarks*: P. dyptocranum* is characterized by thick attachments discs between the cells of a colony (Butterfield et al., 1994; Porter and Riedman, 2016). The specimens from the lower Supergroup do not exhibit those circular thickened discs but bi- or tripartite attachments. They probably constitute a distinct species of *Palaeastrum* but this would need more material for evaluation.

Genus *Satka* Jankauskas, 1979a emended.

Type species: *Satka favosa* Jankauskas, 1979a

Translated Original Diagnosis: "Spherical or oval vesicles, made of separate polygonal or subpolygonal plates, slightly convex outwards. The corner edges of the four-, five- or six- plates are smoothly bent inward, forming a cellular structure (infrastructure) on the inner surface of the vesicle, in the form of ridges up to 1–2 μm in height. On the outer surface of the vesicle, crests correspond to deep grooves. There is no precise external sculpture. The dimensions of the vesicles are 30–60 μm, the plates are 6–8 μm, the thickness of the plates (vesicle walls) is < 1 μm" (Jankauskas et al., 1989).

Emended Diagnosis: Spheroidal or oval organic-walled microfossils, made of large separate and tessellated polygonal, sub-polygonal, quadrate or tetragonal plates. The plates are slightly bent inward forming a vesicle.

Remarks: The genus *Satka* was divided in 6 species, as illustrated by Jankauskas et al. (1989): the type species *S. favosa* and *S. colonialica*; *S. elongata*; *S. granulosa; S. squamifera* and *S. undosa*.

In 2015, Tang and colleagues created the new genus *Squamosphaera* and made a new combination of *Satka colonialica* under this genus. The genus *Satka*, and *S. favosa* its type species, have a wall made of numerous tessellated more or less polygonal platelets clearly visible under SEM and may open by medial split (Javaux et al, 2001, 2003, 2004; Javaux and Knoll, 2016), differing from the continuous wall with numerous bulges that characterized *S. colonialica*. Numerous specimens in the lower Shaler Supergroup have an irregularly shaped vesicle with prominent bulges on the surface (Figs. ??) as opposed to the spheroidal shape and polygonal plates of specimens recognized as *Satka favosa* (Fig. ??). Therefore, we follow here the re-evaluation of Tang et al. (2015) and subsequent emendation by Porter and Riedman (2016) by recognizing *Squamosphaera* as a distinct genus from *Satka*.

Hofmann and Jackson (1994) have suggested that *S. squamifera*, *S. granulosa* and *S. elongata* may constitute taphonomic version of the same senior taxon *S. elongata*. However, *S. favosa* is the senior taxon for species of *Satka*. Subsequently, *Satka elongata* and *S. granulosa* were synonymized with *S. favosa* by Javaux and Knoll (2016) because they do not exhibit clear distinct morphological characters.

Vesicle of *S. squamifera*, as illustrated by Jankauskas et al. (1989)

(pl. 5, Figs. 1, 2, 4 – 7) and Hofmann and Jackson (1994) (figs. 18.19 – 18.23), exhibit a spheroidal or ovoid morphology and rounded or polygonal cellular compartments organized in belt-like rows. Javaux and Knoll (2016) interpreted those cellular compartments as the imprints of cells on an encompassing envelope and suggest the placement of *S. squamifera* under the genus *Squamosphaera.* We agree and transfer them to the genus *Squamosphaera* as *Squamisphaera squamifera* comb. nov. However, the specimens illustrated fig. 18.16 – 18.18, 18.24, 18.25 in Hofmann and Jackson (1994) and plate V, Figs. 3 and 8 in Jankauskas et al. (1989) show clear distinction between "compartments". Moreover, they are similar to specimens from the present work, observed in Grassy Bay and Nelson Head formations (Figs ??). From our observation, it seems that those "compartments" rather represent quadrate or tetragonal tessellated plates. Those specimens, as the specimens from the present material, fit the diagnoses of *Satka favosa*, the type species (spheroidal or ovoid vesicles bearing polygonal or subpolygonal plates) and, therefore, are placed under the name *S. favosa.*

Specimens of *S. undosa* illustrated by Jankauskas et al. (1989) (plate IV, figs. 6, 9) was originally placed in the genus *Symplassiosphaeridium* (Jankauskas, 1979a). However, the specimens seem to represent clusters of small closely packed spheroids, probably of *Synsphaeridium* type, rather than vesicles of *Satka*. Therefore, we disagree with their placement in the genus *Satka*.

The genus was originally polyphyletic as pointed out by Agić et al. (2017), including lobate form (now recognized under the genus *Squamosphaera*) and form made of aggregated polygonal plates (*Satka favosa*). The genus is emended to conform the description of its type species *S. favosa* and to avoid any further taxonomic confusions.

Sakta favosa Jankauskas, 1979a

Fig. 7A – 7D

1979a *Satka favosa* – Jankauskas, pl. 4, Fig. 2.

1989 *Satka favosa* – Jankauskas et al., p. 51, pl. 4, Figs. 1, 2?

1989 *Satka elongata* – Jankauskas et al., p. 51, pl. 4, Figs. 3, 5.

1989 *Satka granulosa* – Jankauskas et al., p. 51, pl. 4, Fig. 8.

1989 *Satka squamifera* – Jankauskas et al., p. 51, pl. 5, Figs. 3, 8.

non 1989 *Satka squamifera* – Jankauskas et al., p. 51, pl. 5, Figs. 1, 2, 4 – 7.

1994 *Satka squamifera* – Hofman and Jackson, p. 28, figs. 18.16 – 18.18, 18.24, 18.25

non 1994 *Satka squamifera* – Hofman and Jackson, p. 28, figs. 18.19 – 18.23.

1994 *Satka* spp. – Hofmann and Jackson, pl. 18, figs. 26–31.

2001 *Satka favosa* – Javaux et al., pl. 1e, f.

2003 *Satka favosa* – Javaux et al., figs. 1–10, 11.

2004 *Satka favosa* – Javaux et al., 2004, p. 125, Fig. 3a–f.

2016 *Satka favosa* Jankauskas, 1979 – Javaux and Knoll, p. 15, figs. 5.6 – 5.9

2017 *Satka favosa* – Adam et al., p. 388, Fig. 2C.

Holotype: Specimen illustrated by Jankauskas in pl. IV, Fig. 2, preparation 16–1815-635, lower and middle Riphean (Mesoproterozoic) successions of the southern Urals, Russia (Jankauskas et al., 1989).

Material: Rare well preserved specimens in Nelson Head (15RAT-T17) and Grassy Bay (RAT-021A1) formations.

Description: Hollow spheroidal and sub-spheroidal vesicles, ranging from 27.0 to 48.9 in diameter (N = 5), with wall made of 2.2 to 16.9 μm (minimum diameter/width; n = 8) polygonal or tetragonal tessellate plates. Excystment by medial split.not observed in the present material.

Remarks: In the present material, specimens assigned to *S. favosa* differ in morphology in Grassy Bay and Nelson Head Formations. Specimens from Nelson Head Fm display polygonal plates with smooth edges and have a large vesicle (Fig. 7A, B) whereas specimens in Grassy Bay Fm are smaller in size and show tetragonal platelets (Fig. 7C, D). The two morphotypes fit the diagnose of *S. favosa.*

Agić et al. (2017) interpreted 3 specimens as *S. granulosa*, a species previously synonymized with *S. favosa* by Javaux and Knoll (2016). Agic et al (2017) described the specimens as having lobe-like edges and suggest they constitute remains of lobate unicellular microorganisms that may belong to a genus distinct of *Satka*. Specimens of the genus *Squamosphaera* are characterized by domical bulges, giving a lobate aspect to the vesicle, and we suggest the specimens of *S. granulosa* (Agić et al., 2017) to be moved to this genus. However, only one specimen is illustrated (fig. 10J) preventing any further taxonomic placement. The specimens could be placed under a new combination (*Squamosphaera granulosa*) or synonymized with *Squamosphaera squamifera* comb. nov.

The wall of *Satka favosa*, made of tessellated plates, suggests it was eukaryotic rather than prokaryotic, as such wall organization is unknown in prokaryotes, and its excystment by medial split shows that was a cyst rather than a vegetative cell (Javaux et al., 2001; 2003; 2004; Javaux and Knoll, 2016).,

Occurrences: Prior to this study *Satka favosa* was restricted to Mesoproterozoic rocks, including the Belt Supergoup in Montana (Adam et al., 2017); the Bylot Supergroup of Arctic Canada (Hofmann and Jackson, 1994), the Roper Group in Australia (Javaux et al, 2001, 2003, 2004; Javaux and Knoll, 2016) as well as the lower and middle Riphean (Mesoproterozoic) successions of the southern Urals (Jankauskas et al., 1989).

Unnamed acanthomorph

Fig. 8R, S

Material: One well-preserved specimen from the Nelson Head Formation (15RAT-T17).

Description: Spheroidal vesicle (37.8 μm in diameter) with ~2.5 μm, small, sturdy dumbbell-shaped processes. The processes are regularly distributed around the vesicle.

Remarks*:* One specimen is recorded, but the consistent shape, size, and distribution of its processes suggest that they do not result from taphonomy but characterize a distinct taxon.

The specimen resembles vesicles of *Galerosphaera walcottii* reported by Porter and Riedman (2016; Fig. 6) from the ca. 750 Ma Chuar Group, but it is not enclosed by an envelope. Moreover, the specimens from the Chuar Group show processes with funnel-shaped distal extremities but with parallel-sided bases. The specimen from the lower Shaler Supergroup shows funnel-shaped distal and basal extremities (dumbbell-like appearance).

Incertae Sedis

Genus *Gyalosphaera* Strother, 1983 (in Strother et al., 1983)

Type species: *Gyalosphaera fluitans* Strother in Strother et al., 1983

Gyalosphaera sp.

Fig. 2M

Material: Five colonies from 15RAT-T17

Description: Colonies, up to 200 μm long, containing spheroidal cells ~1.5 – 3 μm diameter that can be degraded to dark blobs (Strother et al., 1983), loosely distributed in a thin, amorphous matrix.

Remarks: *Gyalosphaera* differs from *Eomicrocystis* Golovenok & Belova (1986) by the presence of a matrix enveloping the vesicles.

The original description of the genus *Gyalosphaera* indicates a spheroidal shape for the colonies with cells located at the periphery. In the present material, they are irregularly shaped but never spheroidal. The original material from Strother et al. (1983) was preserved in chert and described in three dimensions in thin sections. In the present material, the colonies were extracted from shale and are flattened. Therefore, the mucilage surrounding the vesicle, which appears thin and plastic, may have been deformed and crushed, and may have lost its spheroidal shape. On this basis, the present specimens are interpreted as *Gyalosphaera* but are left under open nomenclature.

Genus *Squamosphaera* (Tang et al., 2015) Porter and Riedman, 2016

Type species: *Squamosphaera colonialica* (Jankauskas, 1979b) Tang et al., 2015 emend. Porter and Riedman, 2016

Diagnosis: Single-walled, spheroidal, tomaculate, toroidal, or irregularly shaped vesicles with an irregular outline characterized by numerous broadly domical bulges. Vesicles typically 80–500 μm in maximum dimension; bulges typically 5–30 μm in basal width (emended

from Jankauskas et al. (1979a,b) and Tang et al. (2015) by Porter and Riedman (2016))

Remarks: The genus *Squamosphaera* was erected by Tang et al. (2015) to accommodate taxa originally described as *Satka colonialica* (see above). Porter and Riedman (2016) emended the genus and described *Squamosphaera* vesicles as bearing numerous broadly domical bulges rather than processes as refer to in the original diagnosis.

Vesicles of *Satka squamifera* illustrated by Jankauskas et al. (1989) (plate V, Figs. 1, 2, 4–7) and Hofmann and Jackson (1994) (figs 18.19 – 18.23) exhibit a morphology and bulges on the surface that resemble those of *Squamosphaera* vesicles but with a regularly-shaped vesicle and arrange in belt-like rows. Therefore, we propose the new combination *Squamosphaera squamifera* comb. nov. to accommodate those specimens.

Squamosphaera colonialica (Jankauskas, 1979b) Tang et al., 2015

Fig. 2Q – R

1979b *Satka colonialica* – Jankauskas, p. 192, pl. 1, Figs. 4, 6.

1985 *Satka colonialica* – Knoll and Swett, p. 468, pl. 53, Figs. 4–6, 8.

1989 *Satka colonialica* – Jankauskas et al., p. 51, pl. 4, Figs. 4, 7.

1997 *Satka colonialica* – Samuelsson, p. 175, fig. 9A, B.

1999 *Satka colonialica* – Cotter, p. 77, Fig. 7C.

1999 *Satka colonialica* – Samuelsson et al., Fig. 4G.

2015 *Squamosphaera colonialica* – Tang et al., 2015, p. 312, fig. 12 A–C2, fig. 13 A–F2.

2016 *Squamosphaera colonialica* – Porter and Riedman, fig. 17, 1–7.

2016 *Squamosphaera colonialica* (Jankauskas, 1979) Tang et al., 2015 – Javaux and Knoll, p. 16, fig. 5.14.

Holotype: Specimen number 16-62-4762/22, slide 1. Well Kabakovo-62, 4762-4765 m. Neoproterozoic Zigazino-Komarovo Formation, Ufa, Bashkirian Urals (Jankauskas, 1979b, Fig. 4).

Material: numerous specimens in various state of preservation in 15RAT-021A1; 15RAT-T17; CP15-DD007 140,5m; CP15-DD007 207,2m. Rare specimens in various states of preservation in R37A1 and 15RAT-ER3

Description: Spheroidal, sub-spheroidal, toroidal and irregularly-shaped smooth-walled vesicle with prominent bulges distributed on the wall surface. Irregularly-shaped vesicles are ranging from tens to hundreds μm in size, spheroidal or subspheroidal vesicles are 30 – 110 μm in minimum diameter. Domical bulges are typically < 15 μm in width (N = 10).

Remarks: The morphology of *S. colonialica* with bulges interpreted as imprints of cells on a colonial envelope, suggests a prokaryotic affinity rather than eukaryotic as it resembles pleurocapsalean cyanobacteria (Javaux & Knoll, 2016).

Occurrences: various Mesoproterozoic and Neoproterozoic successions, including the depths of 4,762–4,765 m in Kobakovo-62 drill hole, Ufa, Bashkirian Urals (Jankauskas, 1979b); the Roper Group in Australia (Javaux and Knoll, 2016), the Chuar Group in Arizona (Porter and Riedman, 2016); the Veteranen Group in Svalbard (Knoll and Swett, 1985); the Kildinskaya Group in the Kola Peninsula, Russia (Samuelsson, 1997); Steptoe Formation, Kanpa and Hussar formations, Officer Basin in Australia (Cotter, 1999); the Thule Supergroup in northwest Greenland (Samuelsson et al., 1999); and the Gouhou Formation in Huaibei region, North China (Tang et al., 2015).

Unnamed sphaeromorph

Fig. 2F, G

Material: Around 20 specimens reported from the Nelson Head and Grassy Bay formations.

Description: Ovoidal vesicles with stretched fibrous wall texture, 74.8–79.5 μm wide and 90.5–115.0 μm long (n = 10).

Remarks: Although the vesicles do not show any opening by medial split, they may represent taphonomic variants of *Valeria lophostriata*. Indeed, the "fibers" on the surface may locally be parallel. Similarly, the wall texture may result from taphonomic degradation of the smooth wall of *Leiosphaeridia*. However, the vesicles, found in both Grassy Bay and Nelson Head formations, are identical in morphology and this would be improbable for degraded vesicles.

Specimens commonly display numerous ovoid and circular perforations that have been interpreted as the traces of protists preying on other protists (eukaryovory, Loron et al., 2018).

Unnamed filament

Fig. 3O – Q

2009 remains of large trichome-like forms with narrow cells – Nagovitsin et al., p. 1196, figs. 3.8, 3.17.

Material: around 15 specimens from the Nelson Head Formation.

Description: Association in one plane of 0.5 to 1.6 μm wide filaments aligned parallel and attached together by a thin translucent matrix. Clusters are 15 – 60 μm wide and may contain up to 50 filaments (n = 8).

Remarks: Specimens correspond to clusters of parallel filaments of the type *Syphonophycus septatum*.

Specimens are similar to those reported by Nagovitsin et al. (2009) from the Mesoproterozoic Kamo Group in Siberia (figs. 3.8, 3.17).

Acknowledgements

This research was supported by the Agouron Institute, the FRS-FNRS and the ERC Stg ELiTE FP7/308074. We gratefully thank M. Giraldo (U. Liège) and S. Borensztajn (IPGP) for their technical support, the Geological Survey of Canada's Geomapping for Energy and Minerals Program for the fieldwork logistics and T. Gibson (McGill University) for field assistance during sample collection. We thank Susannah Porter and an anonymous reviewer for their constructive comments.

Appendix A. Supplementary data

Supplementary data to this article can be found online at https://doi.org/10.1016/j.precamres.2018.12.024.

References

Adam, Z.R., Skidmore, M.L., Mogk, D.W., Butterfield, N.J., 2017. A Laurentian record of the earliest fossil eukaryotes. Geology 45 (5), 387–390. https://doi.org/10.1130/G38749.1.

Agić, H., Moczydłowska, M., Yin, L.-M., 2015. Affinity, life cycle, and intracellularcomplexity of organic-walled microfossils from the Mesoproterozoic of Shanxi, China. J. Paleontol. 89, 28–50.

Agić, H., Moczydłowska, M., Yin, L., 2017. Diversity of organic-walled microfossils from the early Mesoproterozoic Ruyang Group, North China Craton-a window into the early eukaryote evolution. Precambr. Res. 297, 101–130. https://doi.org/10.1016/j.precamres.2017.04.042.

Arouri, K., Greenwood, P.F., Walter, M.R., 1999. A possible chlorophycean affinity of some Neoproterozoic acritarchs. Org Geochem. 30 (10), 1323–1337.

Baludikay, B.K., Storme, J.Y., François, C., Baudet, D., Javaux, E.J., 2016. A diverse and exquisitely preserved organic-walled microfossil assemblage from the Meso-Neoproterozoic Mbuji-Mayi Supergroup (Democratic Republic of Congo) and implications for Proterozoic biostratigraphy. Precambr. Res. 281, 166–184. https://doi.org/10.1016/j.precamres.2016.05.017.

Battison, L., Brasier, M.D., 2012. Remarkably preserved prokaryote and eukaryote microfossils within 1 Ga-old lake phosphates of the Torridon Group, NW Scotland. Precambr. Res. 196, 204–217. https://doi.org/10.1016/j.precamres.2011.12.012.

Beghin, J., Storme, J.-Y., Blanpied, C., Gueneli, N., Brocks, J.J., Poulton, S.W., Javaux, E.J., 2017a. Microfossils from the late Mesoproterozoic – early Neoproterozoic Atar/El Mreïti Group, Taoudeni Basin, Mauritania, northwestern Africa. Precambr. Res. 291, 63–82. https://doi.org/10.1016/j.precamres.2017.01.009.

Beghin, J., Guilbaud, R., Poulton, S.W., Gueneli, N., Brocks, J.J., Storme, J.Y., Blanpied, C., Javaux, E.J., 2017b. A palaeoecological model for the late Mesoproterozoic–early Neoproterozoic Atar/El Mreïti Group, Taoudeni Basin, Mauritania, northwestern Africa. Precambr. Res. 299, 1–14.

Bengtson, S., 2002. Origins and early evolution of predation. Paleontological Society Papers 8, 289–318.

Bengtson, S., Sallstedt, T., Belivanova, V. and Whitehouse, M., 2017. Three dimensional preservation of cellular and subcellular structures suggests 1.6 billion-year-old crown-group red algae. PLoS Biol. 15(3), p.e 2000735.

Bosak, T., Lahr, D.J.G., Pruss, S.B., Macdonald, F.A., Dalton, L., Matys, E., 2011a. Agglutinated tests in post-Sturtian cap carbonates of Namibia and Mongolia. Earth Planet. Sci. Lett. 308 (1–2), 29–40.

Bosak, T., Lahr, D.J., Pruss, S.B., Macdonald, F.A., Gooday, A.J., Dalton, L., Matys, E.D., 2012. Possible early foraminiferans in post-Sturtian (716–635 Ma) cap carbonates. Geology 40 (1), 67–70.

Bosak, T., Macdonald, F., Lahr, D., Matys, E., 2011b. Putative cryogenian ciliates from Mongolia. Geology 39 (12), 1123–1126.

Brocks, J.J., Jarrett, A.J., Sirantoine, E., Hallmann, C., Hoshino, Y., Liyanage, T., 2017.

The rise of algae in Cryogenian oceans and the emergence of animals. Nature 548 (7669), 578–581. https://doi.org/10.1038/nature23457.
Butterfield, N.J., 1997. Plankton ecology and the Proterozoic-Phanerozoic transition. Paleobiology 23 (2), 247–262.
Butterfield, N.J., 2000. Bangiomorpha pubescens n. gen., n. sp.: implications for the evolution of sex, multicellularity, and the Mesoproterozoic/Neoproterozoic radiation of eukaryotes. Paleobiology 26 (3), 386–404. https://doi.org/10.1666/0094-8373(2000)026<0386:BPNGNS>2.0.CO;2.
Butterfield, N.J., 2004. A vaucheriacean alga from the middle Neoproterozoic ofSpitsbergen: implications for the evolution of Proterozoic eukaryotes and theCambrian explosion. Paleobiology 30, 231–252.
Butterfield, N.J., 2005a. Probable Proterozoic fungi. Paleobiology 31, 165–182.
Butterfield, N.J., 2005b. Reconstructing a complex early Neoproterozoic eukaryote, Wynniatt Formation, arctic Canada. Lethaia 38, 155–169. https://doi.org/10.1080/00241160510013231.
Butterfield, N.J., 2009. Modes of pre-Ediacaran multicellularity. Precambr. Res. 173 (1–4), 201–211.
Butterfield, N.J., 2015a. Early evolution of the Eukaryota. Palaeontology 58 (1), 5–17.
Butterfield, N.J., 2015b. Proterozoic photosynthesis–a critical review. Palaeontology 58 (6), 953–972.
Butterfield, N.J., Knoll, A.H., Swett, K., 1994. Paleobiology of the Neoproterozoic Svanbergfjellet Formation, Spitsbergen. Fossils Strata 34, 1–84.
Butterfield, N.J., Rainbird, R.H., 1998. Diverse organic-walled fossils, including “possible dinoflagellates”, from the early Neoproterozoic of arctic Canada. Geology 26 (11), 963–966. https://doi.org/10.1130/0091-7613(1998) 026<0963:DOWFIP> 2.3.CO;2.
Cohen, P.A., Macdonald, F.A., 2015. The Proterozoic Record of Eukaryotes. Paleobiology 41 (4), 1–23. https://doi.org/10.1017/pab.2015.25.
Cohen, P.A., Riedman, L.A., 2018. It's a protist-eat-protist world: recalcitrance, predation, and evolution in the Tonian–Cryogenian ocean. Emerging Topics Life Sci. p. ETLS20170145. https://doi.org/10.1042/ETLS20170165.
Cohen, P.A., Schopf, J.W., Butterfield, N.J., Kudryavtsev, A.B., Macdonald, F.A., 2011. Phosphate biomineralization in mid-Neoproterozoic protists. Geology 39 (6), 539–542.
Cotter, K.L., 1999. Microfossils from neoproterozoic supersequence 1 of the officer basin, Western Australia. Alcheringa 23 (2), 63–86.
Eisenack, A., 1958. Tasmanites Newton 1875 und Leiosphaeridia n. gen. aus Gattungender Hystrichosphaeridea. Palaeontographica Abteilung A 110, 1–19.
François, C., Baludikay, B.K., Storme, J.Y., Baudet, D., Paquette, J.L., Fialin, M., Javaux, E.J., 2017. Contributions of U-Th-Pb dating on the diagenesis and sediment sources of the lower group (BI) of the Mbuji-Mayi Supergroup (Democratic Republic of Congo). Precambr. Res. 298, 202–219.
Gibson, T.M., Shih, P.M., Cumming, V.M., Fischer, W.W., Crockford, P.W., Hodgskiss, M. S., Wörndle, S., Creaser, R.A., Rainbird, R.H., Skulski, T.M., Halverson, G.P., 2017. Precise age of Bangiomorpha pubescens dates the origin of eukaryotic photosynthesis. Geology, published online in December 2017, doi: 10.1130/G39829.1.
Golovenok, M.K., Belova, M.Y., 1986. The Riphean microflora in the cherts from the Malgin Formation in the Yudoma-Maya basin. Paleontolog. J. 2, 85–90.
Golub, I.N., 1979. A new group of problematic microstructures in Vendian depositsof the Orshanka Basin (Russian Platform). In: Sokolov, S.B. (Ed.), PaleontologiyaDokembriya i Rannego Kembriya. Nauka, Leningrad, pp. 147–155.
Greenman, J.W., Rainbird, R.H., 2018. Stratigraphy of the upper Nelson Head, Aok, Grassy Bay, and Boot Inlet formations in the Brock Inlier, Northwest Territories (NTS 97-A, D). Geological Survey Open File 8394.
Grey, K., 1999. A modified palynological preparation technique for the extraction of large Neoproterozoic acanthomorph acritarchs and other acid insoluble microfossils. Record-Geological Survey of Western Australia 199 (10), 1–23.
Heaman, L.M., LeCheminant, A.N., Rainbird, R.H., 1992. Nature and timing of Franklin igneous events, Canada: implications for a Late Proterozoic mantle plume and the break-up of Laurentia. Earth Planet. Sci. Lett. 109, 117–131.
Hermann, T.N., 1974. Findings of mass accumulations of trichomes in the Riphean. In: Timofeev, B.V. (Ed.), Proterozoic and Paleozoic Microfossils of the USSR. Nauka, Moscow, pp. 6–10.
Hermann, T.N., 1981. Filamentous microorganisms in the Lakhanda Formation onthe Maya River. Paleontol. J. 1981 (2), 126–131 (100–107 in English translation).
Hermann, T.N., 1990. Organic World Billion Year Ago. Nauka, Leningrad.
Hermann, T.N., Timofeev, B.V., 1985. Eosolenides—a New Group of Late Precambrian Problematic Organisms. Problematics of the Late Precambrian and Paleozoic 37–40.
Hofmann, H.J., 1976. Precambrian Microflora, Belcher Islands, Canada: significanceand systematics. J. Paleontol. 50, 1040–1073.
Hofmann, H.J., 1985. The mid-Proterozoic Little Dal macrobiota, Mackenzie Mountains, north-west Canada. Palaeontology 28 (2), 331–354.
Hofmann, H.J., Aitken, J.D., 1979. Precambrian biota from the Little Dal Group, Mackenzie Mountains, northwestern Canada. Can. J. Earth Sci. 16, 150–166.
Hofmann, H.J., Jackson, G.D., 1994. Shale-facies microfossils from the ProterozoicBylot Supergroup, Baffin Island, Canada. Paleontol. Soc. Mem. 37, 1–35.
Hofmann, H.J., Rainbird, R.H., 1994. Carbonaceous megafossils from the Neoproterozoic Shaler Supergroup of Arctic Canada. Palaeontology 37 (4), 721–732.
Huntley, J.W., Xiao, S., Kowalewski, M., 2006. 1.3 Billion years of acritarch history: an empirical morphospace approach. Precambr. Res. 144 (1–2), 52–68.
Jankauskas, T.V., 1979a. Lower Riphean microbiotas of the Southern Urals. Akademiya Nauk SSSR Doklady [Proceedings of the USSR Academy of Sciences], 247, 1465–1467 (51–54 in English translation).
Jankauskas, T.V., 1979. Srednerifeyski microbiota Yuzhnogo Urala I Bashkirskogo Priural'ya [Middle Riphean microbiota of the southern Urals and the Ural region in Bashkiria]: Akademii Nauk SSSR. Doklady [Proceedings of the USSR Academy of Sciences] 248, 190–193 [in Russian].
Jankauskas, T.V., 1982. Microfossils of the Riphean of the South Urals, the RipheanStratotype, Paleontology, Paleomagnitism. Akademia Nauk SSSR, Moscow, pp. 84–120.
Jankauskas, T.V., Mikhailova, N.S., Hermann, T.N. (Eds.), 1989. Precambrian Microfossils of the USSR. Nauka, Leningrad.
Javaux, E.J., 2006. The early eukaryote fossil record. In: Jékely, Gáspár (Ed.), Evolution of the Eukaryotic Endomembrane System and Cytoskeleton. Landes Biosciences Publishers, Texas, USA, pp. 19.
Javaux, E.J., 2011. Early eukaryotes in Precambrian oceans. In: Gargaud, M., López-Garcìa, P., Martin, H. (Eds.), Origins and evolution of life: an astrobiological perspective. Cambridge University Press, Cambridge, pp. 411–449.
Javaux, E.J., Knoll, A.H., 2016. Micropaleontology of the lower Mesoproterozoic Roper Group, Australia, and implications for early eukaryotic evolution. J. Palaeontol. 91 (2), 199–229. https://doi.org/10.1017/jpa.2016.124.
Javaux, E.J., Knoll, A.H., Walter, M.R., 2001. Morphological and ecological complexity in early eukaryotic ecosystems. Nature 412 (6842), 66.
Javaux, E.J., Knoll, A.H., Walter, M., 2003. Recognizing and interpreting the fossils of early eukaryotes. Orig. Life Evol. Biosph. 33 (1), 75–94.
Javaux, E.J., Knoll, A.H., Walter, M.R., 2004. TEM evidence for eukaryotic diversity in mid-Proterozoic oceans. Geobiology 2 (3), 121–132.
Javaux, E.J., Lepot, K., 2017. The Paleoproterozoic fossil record: Implications for the evolution of the biosphere during Earth's middle-age. Earth Sci. Rev. 176, 68–86. http://doi.org/ 10.1016/j.earscirev .2017.10.001.
Knoll, A.H., 1994. Proterozoic and Early Cambrian protists: evidence for accelerating evolutionary tempo. Proc. Natl. Acad. Sci. 91 (15), 6743–6750.
Knoll, A.H., 2015. Paleobiological perspectives on early eukaryotic evolution. Cold Spring Harbor Perspect. Biol. 6, a016121. https://doi.org/10.1101/cshperspect.a016121.
Knoll, A.H., Swett, K., 1985. Micropalaeontology of the late proterozoic veteranen group, spitsbergen. Palaeontology 28 (3), 451–473.
Knoll, A.H., Javaux, E.J., Hewitt, D., Cohen, P., 2006. Eukaryotic organisms in Proterozoic oceans. Philos. Trans. R. Soc. B Biol. Sci. 361, 1023–1038. https://doi.org/10.1098/rstb.2006.1843.
Knoll, A.H., Lahr, D.J., Niklas, K.J., Newman, S., Bonner, J.T., 2016. Fossils, feeding, and the evolution of complex multicellularity. In: Multicellularity, Origins and Evolution, The Vienna Series in Theoretical Biology. Massachusetts Institute of Technology, Boston, pp. 1–16.
Knoll, A.H., Swett, K., Mark, J., 1991. Paleobiology of a Neoproterozoic tidalflat/lagoonal complex: the Draken Conglomerate Formation, Spitsbergen. J. Paleontol. 65, 531–570.
Kolosov, P.N., 1984. Upper Precambrian microorganisms from the east of Siberian Platform. Yakutskii Filial Sibirskogo Otdeleniya AN SSSR.
LeCheminant, A.N., Heaman, L.M., 1989. Mackenzie igneous events, Canada: Middle Proterozoic hotspot magmatism associated with ocean opening. Earth Planet. Sci. Lett. 96, 38–48. https://doi.org/10.1016/0012 -821X (89)90122 -2.
Lenton, T.M., Boyle, R.A., Poulton, S.W., Shields-Zhou, G.A., Butterfield, N.J., 2014. Co-evolution of eukaryotes and ocean oxygenation in the Neoproterozoic era. Nat. Geosci. 7 (4), 257.
Long, D.G.F., Rainbird, R.H., Turner, E.C., MacNaughton, R.B., 2008. Early Neoproterozoic strata (Sequence B) of mainland northern Canada and Victoria and Banks islands: a contribution to the Geological Atlas of the Northern Canadian Mainland Sedimentary Basin. Geological Survey of Canada, Open File 5700 (2008), 1–27.
Loron, C., Moczydłowska, M., 2017. Tonian (Neoproterozoic) eukaryotic and prokaryotic organic-walled microfossils from the upper Visingsö Group, Sweden. Palynology 42 (2), 220–254.
Loron, C.C., Rainbird, R.H., Turner, E.C., Greenman, J.W., Javaux, E.J., 2018, Implications of selective predation on the macroevolution of eukaryotes: evidence from Arctic Canada. Emerging Topics Life Sci. p. ETLS20170153. https://doi.org/10.1042/ETLS20170153.
Lyons, T.W., Reinhard, C.T., Planavsky, N.J., 2014. The rise of oxygen in Earth's early ocean and atmosphere. Nature 506 (7488), 307.
Macdonald, F.A., Schmitz, M.D., Crowley, J.L., Roots, C.F., Jones, D.S., Maloof, A.C., Strauss, J.V., Cohen, P.A., Johnston, D.T., Schrag, D.P., 2010. Calibrating the cryogenian. Science 327 (5970), 1241–1243.
Maithy, P.K., 1975. Micro-organisms from the Bushimay System (Late Precambrian) of Kanshi, Zaire. The Palaeobotanist 22, 133–147.
Marshall, C.P., Javaux, E.J., Knoll, A.H., Walter, M.R., 2005. Combined micro-Fourier transform infrared (FTIR) spectroscopy and micro-Raman spectroscopy of Proterozoic acritarchs: a new approach to palaeobiology. Precambr. Res. 138 (3–4), 208–224.
Mikhailova, N.S., 1986. New finds of microphytofossils from upper Riphean depositsof the Krasnoyar region. In: Sokolov, B.S. (Ed.), Current Questions of Contempo-rary Palaeoalgology. Naukova Dumka, Kiev, pp. 31–37.
Moczydłowska, M., 2008. The Ediacaran microbiota and the survival of Snowball Earth conditions. Precambr. Res. 167 (1–2), 1–15.
Moczydłowska, M., 2016. Algal affinities of Ediacaran and Cambrian organic-walled microfossils with internal reproductive bodies: Tanarium and other morphotypes. Palynology 40 (1), 83–121.
Moczydłowska, M., Landing, E.D., Zang, W., Palacios, T., 2011. Proterozoic phytoplankton and timing of chlorophyte algae origins. Palaeontology 54 (4), 721–733.
Moczydłowska, M., Willman, S., 2009. Ultrastructure of cell walls in ancient microfossils as a proxy to their biological affinities. Precambr. Res. 173 (1–4), 27–38.
Morais, L., Fairchild, T.R., Lahr, D.J., Rudnitzki, I.D., Schopf, J.W., Garcia, A.K., Kudryavtsev, A.B., Romero, G.R., 2017. Carbonaceous and siliceous Neoproterozoic vase-shaped microfossils (Urucum Formation, Brazil) and the question of early protistan biomineralization. J. Paleontol. 91 (3), 393–406.
Nagovitsin, K., 2009. Tappania-bearing association of the Siberian platform: bio-diversity, stratigraphic position and geochronological constraints. Precambr. Res. 173, 137–145.
Naumova, S.N., 1949. Spores from the Lower Cambrian. Izvestiya Akademii NaukSSSR, Seriya Geologicheskaya 1949 (4), 49–56.
Niklas, K.J., 2000. The evolution of plant body plans—a biomechanical perspective. Ann. Botany London 85, 411–438.
Ouyang, S., 1974. Acritarch fossils of the Sinian System of southeast China. Handbook of

Stratigraphy and Paleontology of Southwest China, Nanjing Inst. Geol. Palaeontol., Acad. Sinica. Scientific Press, Beijing, 72–79.
Peng, Y., Bao, H., Yuan, X., 2009. New morphological observations for Paleoproterozoic acritarchs from the Chuanlinggou Formation, North China. Precambr. Res. 168 (3–4), 223–232.
Planavsky, N.J., Reinhard, C.T., Wang, X., Thomson, D., McGoldrick, P., Rainbird, R.H., Johnson, T., Fischer, W.W., Lyons, T.W., 2014. Low Mid-Proterozoic atmospheric oxygen levels and the delayed rise of animals. Science 346 (6209), 635–638.
Porter, S., 2011. The rise of predators. Geology 39 (6), 607–608.
Porter, S.M., 2016. Tiny vampires in ancient seas: evidence for predation via perforation in fossils from the 780–740 million-year-old Chuar Group, Grand Canyon, USA. 20160221. Proc. R. Soc. B 283. https://doi.org/10.1098/rspb.2016.0221.
Porter, S.M., Knoll, A.H., 2000. Testate amoebae in the Neoproterozoic Era: evidence from vase-shaped microfossils in the Chuar Group, Grand Canyon. Paleobiology 26 (3), 360–385.
Porter, S.M., Meisterfeld, R., Knoll, A.H., 2003. Vase-shaped microfossils from the Neoproterozoic Chuar Group, Grand Canyon: a classification guided by modern testate amoebae. J. Paleontol. 77 (3), 409–429.
Porter, S.M., Riedman, L.A., 2016. Systematics of organic-walled microfossils from the ca. 780–740 Ma Chuar Group, Grand Canyon, Arizona. J. Paleontol. 90 (5), 815–853.
Pyatiletov, V.G., 1980. Yudoma complex microfossils from southern Yakutia. Geol. Geofiz. 7, 8–20.
Rainbird, R.H., Heaman, L.M., and Young, G.M., 1992. Sampling Laurentia: Detrital zircon geochronology offers evidence for an extensive Neoproterozoic river system originating from Grenville orogeny. Geology 20, 351–354, doi: 10.1130 /0091 -7613 (1992)020 < 0351: SLDZGO > 2 .3 .CO;2.
Rainbird, R.H., Jefferson, C.W., Hildebrand, R.S., and Worth, J.K., 1994, The Shaler Supergroup and revision of Neoproterozoic stratigraphy in the Amundsen Basin, Northwest Territories: Geological Survey of Canada Current Research 1994-C, pp. 61–70, doi: 10 .4095 /193814.
Rainbird, R.H., Jefferson, C.W., Young, G.M., 1996. The early Neoproterozoic sedimentary Succession B of northwestern Laurentia: correlations and paleogeographic significance. Geol. Soc. Am. Bull. 108 (4), 454–470.
Rainbird, R.H., Rayner, N.M., Hadlari, T., Heaman, L.M., Ielpi, A., Turner, E.C., MacNaughton, R.B., 2018. Zircon provenance data record lateral extent of a pan-continental, early Neoproterozoic river system and erosional unroofing history of the Grenvillian orogeny. Geol. Soc. Am. Bull. 129 (11–12), 1408–1423. https://doi.org/10.1130/B31695.1.
Rayner, N.M., Rainbird, R.H., 2013. U-Pb Geochronology of the Shaler Supergroup, Victoria Island, Northwest Canada: 2009–2013. Geological Survey of Canada Open File 7419, 62. https://doi.org/10.4095/292694.
Riedman, L.A., Porter, S.M., Halverson, G.P., Hurtgen, M.T., Junium, C.K., 2014. Organic-walled microfossil assemblages from glacial and interglacial Neoproterozoic units of Australia and Svalbard. Geology 42 (11), 1011–1014.
Riedman, L.A., Porter, S., 2016. Organic-walled microfossils of the mid-Neoproterozoic Alinya Formation, Officer Basin, Australia. J. Paleontol. 90 (5), 854–887.
Riedman, L.A., Porter, S.M., Calver, C.R., 2018. Vase-shaped microfossil biostratigraphy with new data from Tasmania, Svalbard, Greenland, Sweden and the Yukon. Precambr. Res. 319, 19–36. https://doi.org/10.1016/j.precamres.2017.09.019.
Riedman, L.A., Sadler, P.M., 2017. Global species richness record and biostratigraphic potential of early to middle Neoproterozoic eukaryote fossils. Precambr. Res. published online in October 2017, doi: 10.1016/j.precamres.2017.10.008.
Rooney, A.D., Austermann, J., Smith, E.F., Li, Y., Selby, D., Dehler, C.M., Schmitz, M.D., Karlstrom, K.E., Macdonald, F.A., 2017. Coupled Re-Os and U-Pb geochronology of the Tonian Chuar Group, Grand Canyon. Geol. Soc. Am. Bull. 130 (7–8), 1085–1098.
Samuelsson, J., 1997. Biostratigraphy and palaeobiology of early Neoproterozoic strata of the Kola Peninsula, Northwest Russia. Norsk Geol. Tidsskr. 77 (3), 165–192.
Samuelsson, J., Dawes, P.R., Vidal, G., 1999. Organic-walled microfossils from the Proterozoic Thule Supergroup, northwest Greenland. Precambrian Res. 96 (1–2), 1–23.
Schopf, J.W., 1968. Microflora of the Bitter Springs Formation, Late Precambrian, central Australia. J. Paleontol. 42, 651–688.
Schopf, J.W., Blacic, J.M., 1971. New microorganisms from the Bitter Springs Formation (late Precambrian) of the north-central Amadeus Basin, Australia. J. Paleontol. 45 (6), 925–960.
Seong-Joo, L., Golubic, S., 1998. Multi-trichomous cyanobacterial microfossils from the Mesoproterozoic Gaoyuzhuang Formation, China: paleoecological and taxonomic implications. Lethaia 31, 169–184.
Sergeev, V.N., Knoll, A.H., Vorob'eva, N.G., Sergeeva, N.D., 2016. Microfossils from the lower Mesoproterozoic Kaltasy Formation, East European Platform. Precambr. Res. 278, 87–107.
Sergeev, V.N., Sharma, M., Shukla, Y., 2012. Proterozoic fossil cyanobacteria. Palaeobotanist 61, 189–358.
Shepeleva, E.D., 1960. Nakhodki sinezelenykh vodoroslej v nizhnekembrijskikh otlozheniyakh Leningradskoj oblasti [Finds of blue-green algae in Lower Cambrian deposits of the Leningrad region]. in., Problemy Neftyanoj Geologii i Voprosy Metodiki Laboratornykh Issledovanij. Problemy Neftyanoj Geologii i Voprosy Metodiki Laboratornykh Issledovanij. Nauka, Moscow, pp. 170–172.
Shepeleva, E.D., 1974. Stratigraphic subdivisions of Venedian deposits of the Central Russian platform from acritarchs. Izvestiya Akademii Nauk SSSR, Novosobrisk 81, 13–23.
Staplin, F.L., Jansonius, J., Pocock, S.A., 1965. Evaluation of some acritarchous hystrichosphere genera. Neues Jb. Geol. Paläontol. Abh. 123 (2), 167–201.
Strother, P.K., Battison, L., Brasier, M.D., Wellman, C.H., 2011. Earth's earliest non-marine eukaryotes. Nature 473 (7348), 505.
Strother, P.K., Knoll, A.H., Barghoorn, E.S., 1983. Micro-organisms from the late Precambrian Narssarssuk Formation, northwestern Greenland. Palaeontology 26, 1–32.
Strother, P.K., Wellman, C.H., 2016. Palaeoecology of a billion-year-old non-marine cyanobacterium from the Torridon Group and Nonesuch Formation. Palaeontology 59 (1), 89–108.
Stüeken, E.E., Bellefroid, E., Prave, A.R., Asael, D., Planavsky, N., Lyons, T., 2017. Not so non-marine? Revisiting the Stoer Group and the Mesoproterozoic biosphere. Geochem. Perspect. Lett. 3 (2), 221–229. https://doi.org/10.7185/geochemlet.1725.
Talyzina, N.M., Moczydowska, M., 2000. Morphological and ultrastructural studies of some acritarchs from the Lower Cambrian Lükati Formation, Estonia. Rev. Palaeobotany Palynol. 112 (1–3), 1–21.
Tang, Q., Pang, K., Xiao, S., Yuan, X., Ou, Z., Wan, B., 2013. Organic-walled microfos-sils from the early Neoproterozoic Liulaobei Formation in the Huainan regionof North China and their biostratigraphic significance. Precambr. Res. 236, 157–181.
Tang, Q., Pang, K., Yuan, X., Wan, B., Xiao, S., 2015. Organic-walled microfossils from the Tonian Gouhou Formation, Huaibei region, North China Craton, and their biostratigraphic implications. Precambr. Res. 266, 296–318.
Tang, Q., Hughes, N.C., McKenzie, N.R., Myrow, P.M., Xiao, S., 2017. Late Mesoproterozoic–early Neoproterozoic organic-walled microfossils from the Madhubani Group of the Ganga Valley, northern India. Palaeontology 60 (6), 869–891.
Tappan, H.N., 1980. The paleobiology of plant protists. WH Freeman.
Timofeev, B.V., 1966. Micropaleophytological Investigations of Ancient Formations. Nauka, Moscow, pp. 1–237.
Timofeev, B.V., 1969. Proterozoic Spheromorphida. Nauka, Leningrad.
Timofeev, B.V., Hermann, T.N., 1979. Precambrian microbiota of the LakhandaFormation. In: Sokolov, B.S. (Ed.), Paleontology of the Precambrian and EarlyCambrian. Nauka, Leningrad, pp. 137–147.
Timofeev, B.V., Hermann, T.N., Mikhailova, N.S., 1976. Microphytofossils of the Precambrian, Cambrian and Ordovician. Nauka, Leningrad, pp. 1–106.
Van Acken, D., Thomson, D., Rainbird, R.H., Creaser, R.A., 2013. Constraining the depositional history of the Neoproterozoic Shaler Supergroup, Amundsen Basin, NW Canada: Rhenium-osmium dating of black shales from the Wynniatt and Boot Inlet Formations. Precambr. Res. 236, 124–131. https://doi.org/10.1016/j.precamres.2013.07.012.
Vidal, G., 1976. Late Precambrian microfossils from the Visingso Beds in southern Sweden. Universitetsforlaget.
Vidal, G., Ford, T.D., 1985. Microbiotas from the late Proterozoic Chuar Group (north-ern Arizona) and Uinta Mountain Group (Utah) and their chronostratigraphic implications. Precambr. Res. 28, 349–389.
Vidal, G., Moczydłowska-Vidal, M., 1997. Biodiversity, speciation, and extinction trends of Proterozoic and Cambrian phytoplankton. Paleobiology 23 (2), 230–246.
Vidal, G., Siedlecka, A., 1983. Planktonic, acid-resistant microfossils from the upper Proterozoic strata of the Barents Sea region of Varanger Peninsula, East Finnmark, Northern Norway. Norges Geologiske Undersokelse Bulletin 71, 45–79.
Vorob'eva, N.G., Sergeev, V.N., Petrov, P.Y., 2015. Kotuikan Formation assemblage: a diverse organic-walled microbiota in the Mesoproterozoic Anabar succession, northern Siberia. Precambr. Res. 256, 201–222.
Walcott, C.D., 1899. Pre-Cambrian fossiliferous formations. Bull. Geol. Soc. Am. 10, 199–244.
Willman, S., 2009. Morphology and wall ultrastructure of leiosphaeric and acanto-morphic acritarchs from the Ediacaran of Australia. Geobiology 7, 8–20.
Woese, C.R., Kandler, O., Wheelis, M.L., 1990. Towards a natural system of organisms: proposal for the domains Archaea, Bacteria, and Eucarya. Proc. Natl. Acad. Sci. 87 (12), 4576–4579.
Xiao, S., Dong, L., 2006. On the morphological and ecological history of Proterozoic macroalgae. In Neoproterozoic Geobiology and Paleobiology. Springer, Dordrecht, pp. 57–90.
Xiao, S., Tang, Q., 2018. After the boring billion and before the freezing millions: evolutionary patterns and innovations in the Tonian Period. Emerging Topics Life Sci. p. ETLS20170165. https://doi.org/10.1042/ETLS20170165.
Xiao, S., Muscente, A.D., Chen, L., Zhou, C., Schiffbauer, J.D., Wood, A.D., Polys, N.F., Yuan, X., 2014. The Weng'an biota and the Ediacaran radiation of multicellular eukaryotes. Natl. Sci. Rev. 1 (4), 498–520.
Xing, Y., Liu, G., 1973. Sinian micropaleoflora in the Yan-Liao area and its geologi-calsignificance. Acta Geol. Sin. 1973 (1), 1–31.
Yin, L.M., 1997. Acanthomorphic acritarchs from Meso-Neoproterozoic shales of the Ruyang Group, Shanxi, China. Rev. Palaeobotany Palynol. 98 (1–2), 15–25.
Yin, L.M., Xunlai, Y., Fanwei, M., Jie, H., 2005. Protists of the Upper Mesoproterozoic Ruyang Group in Shanxi Province, China. Precambr. Res. 141 (1–2), 49–66.
Young, G.M., Jefferson, C.W., Delaney, G.D., Yeo, G.M., 1979. Middle and upper proterozoic evolution of the northern cordillera and shield. Geology 7, 125–128.
Young, G.M., 1981. The Amundsen embayment, North-west Territories: relevance to the upper Proterozoic evolution of North America. In: Campbell, F.H.A. (Ed.), Proterozoic basins of Canada. Geological Survey of Canada, pp. 203–218.
Zang, W.L., 1995. Early Neoproterozoic sequence stratigraphy and acritarchbiostratigraphy, eastern Officer Basin, South Australia. Precambr. Res. 74, 119–175.